# Recent results from NA61/SHINE

**Seweryn Kowalski**
**for the NA61/SHINE Collaboration**
**University of Silesia, Katowice**

# NA61/SHINE – few facts

- Located at the CERN SPS
- Successor of NA49
- Large acceptance spectrometer for fixed target experiment on primary (ions) and secondary (ions, hadrons) beams
- Data taking since 2009

# Physics program

- **Strong interactions program**
  - **search for the critical point of strongly interacting matter**
  - **study of the properties of the onset of deconfinement**
  - **study high $p_T$ particles production (energy dependence of nuclear modification factor)**
- Hadron-production measurements for neutrino experiments
  - reference measurements for the neutrino experiment  for computing initial neutrino fluxes at J-PARC, FERMILAB
- Hadron-production measurements for cosmic ray experiments
  - reference measurements of p+C, p+p, $\pi$+C, and K+C interactions for cosmic-ray physics (Pierre-Auger, KASCADE) for improving air shower simulations

# NA61/SHINE 2D scan goals

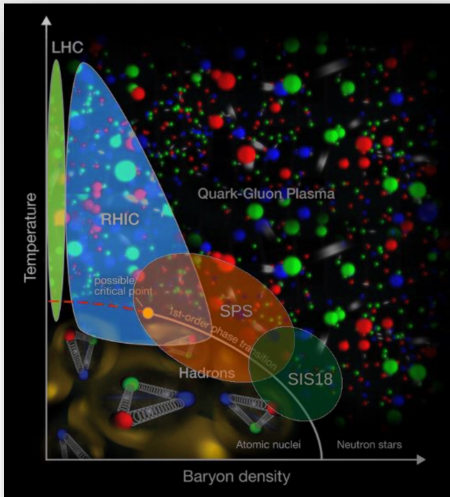


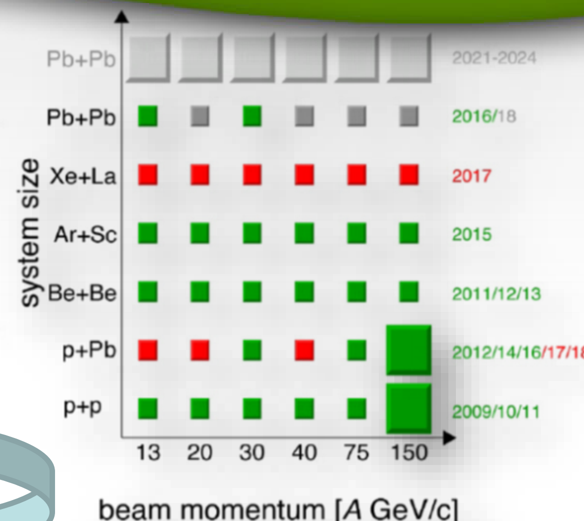


Statistical Model of the Early Stage (SMES)

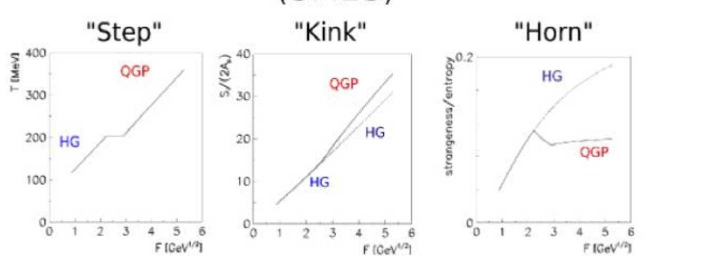


$F \approx \sqrt[4]{s_{NN}}$

Gaździcki, Gorenstein, Acta Phys. Polon. B30, 2705 (1999)

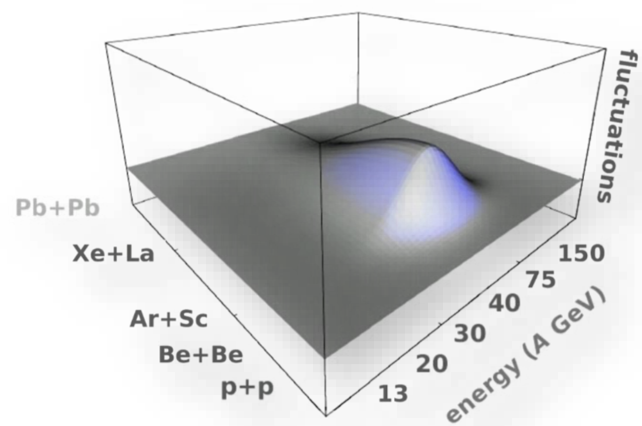

# Facility

# Beams for NA61/SHINE

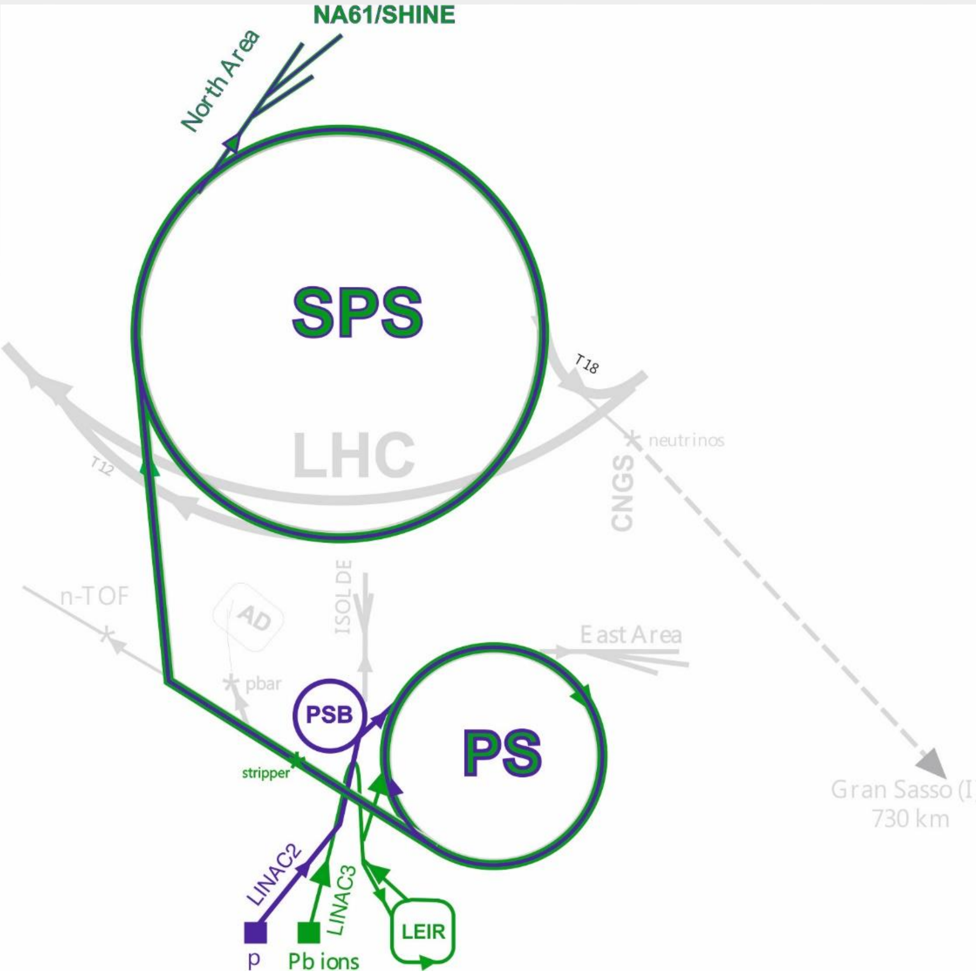


Available beams:

- Primary ions (13A - 150A GeV/c):
  - Argon
  - Xenon
  - Lead
- Secondary:
  - hadrons (p,$\pi^{\pm}$, K$^{\pm}$) 13 - 350 GeV/c
  - ions (Be, . . . ) 13A - 150A GeV/c

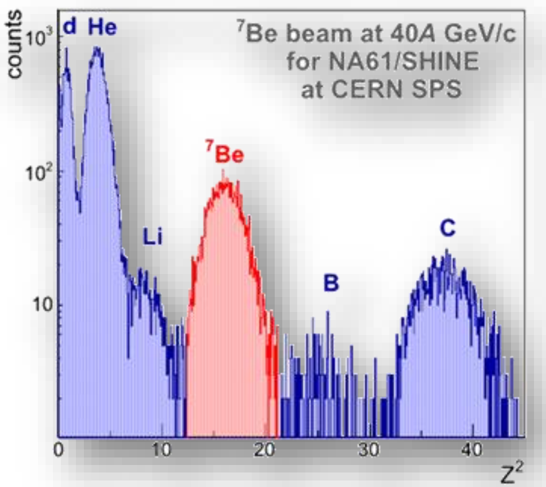


Secondary ion beam composition
(Pb fragmentation on Be target)

# Experimental layout

Unique, multi-purpose facility to study hadron production in hadron-proton, hadron-nucleus and nucleus-nucleus collisions at the CERN SPS

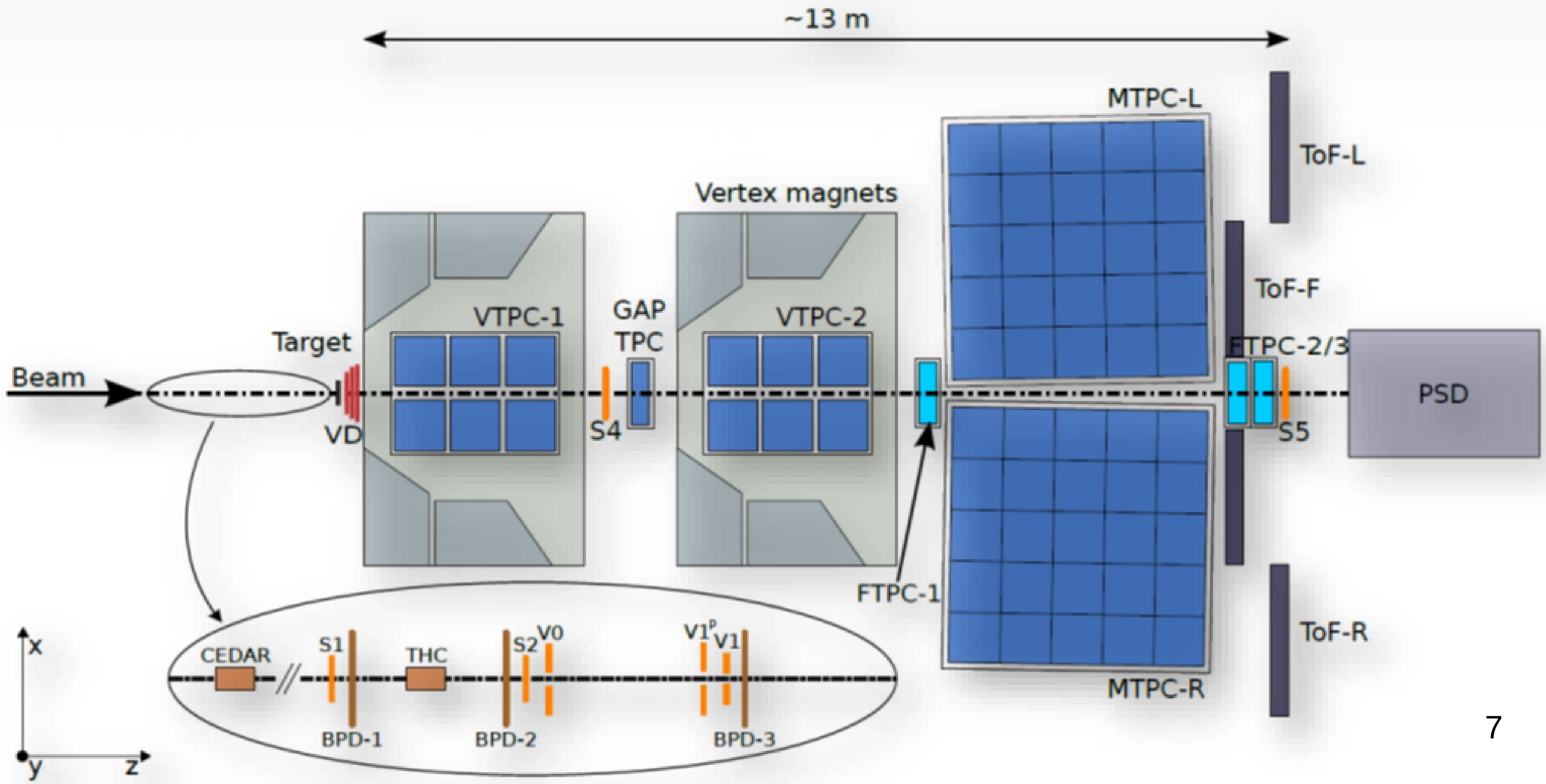

# Particle identification

- $h^-$ analysis based on the fact that the majority of negatively charged particles are $\pi^-$ mesons. Contribution of the other particles is subtracted using EPOS Monte-Carlo
- dE/dx analysis uses TPC energy loss information to identify particles
- tof-dE/dx method estimates number of $p$, K, $\pi$ using an energy loss and a particle time of flight measurements

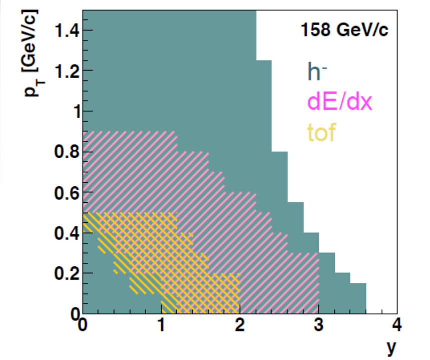


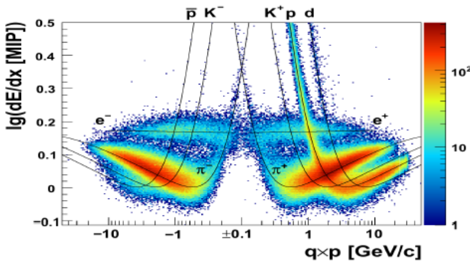


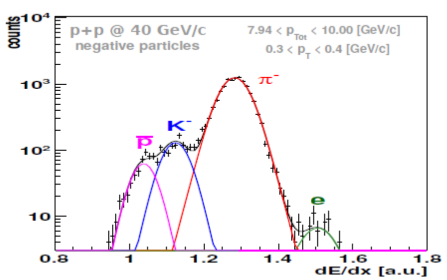


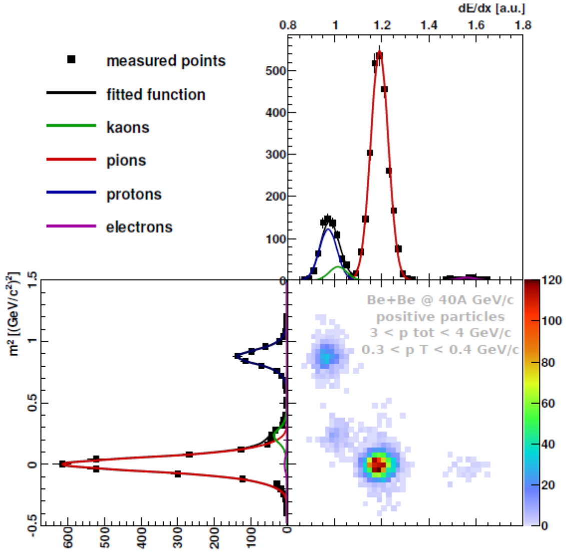

# Event selection

- Use PSD calorimeter
- Based on forward energy measurements (reaction violence selection)
- The forward energy ($E_F$) is dominated by energy of projectile spectators

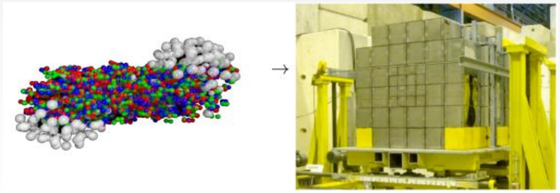

**Ar+Sc – example**

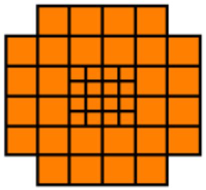

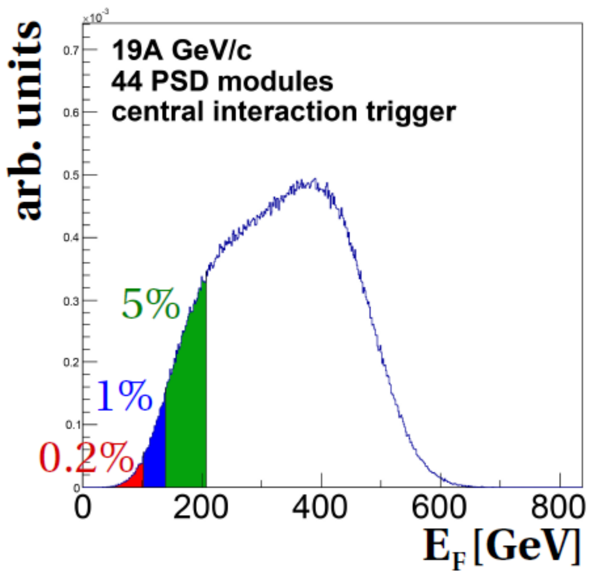


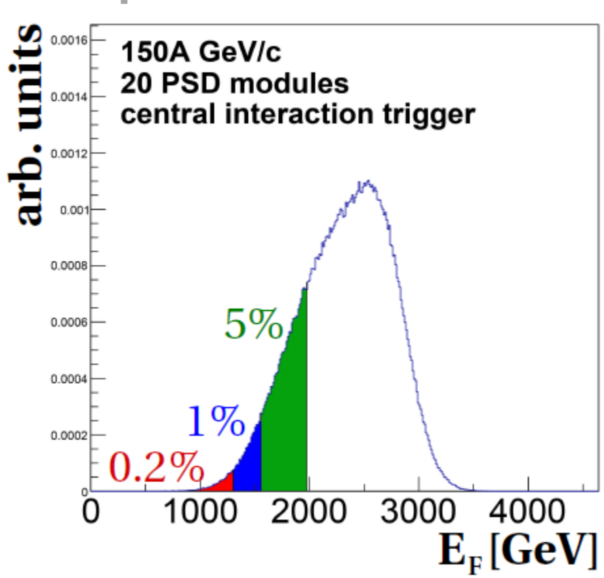


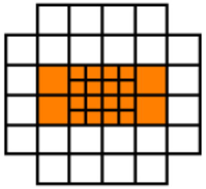

# Onset of deconfinement

# $\pi^-$ spectra from 2D-scan

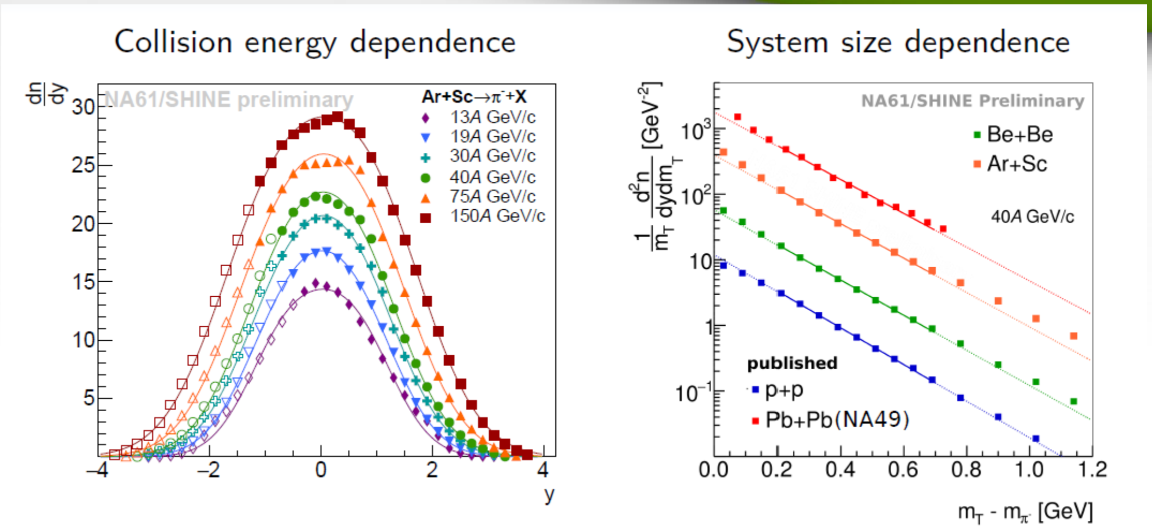


- Rapidity spectra approximately Gaussian, independently of the collision energy and system size
- Large acceptance allows to obtain $4\pi$ multiplicity (sum of data and extrapolation, for details see arXiv:1612.01334)
- $m_T$ spectra in p+p exponential
- $m_T$ spectra in larger systems (central collisions) deviate from the exponential shape

# Energy and system size dependence of $m_T$ spectra

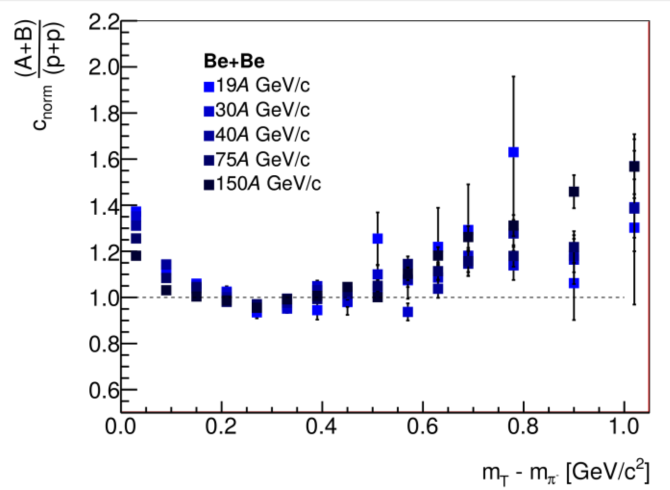


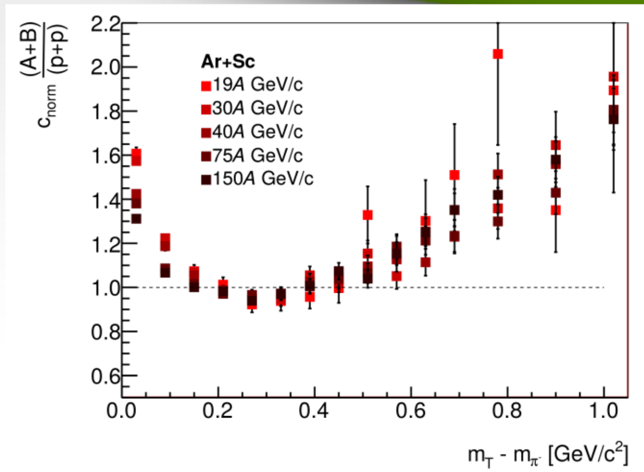


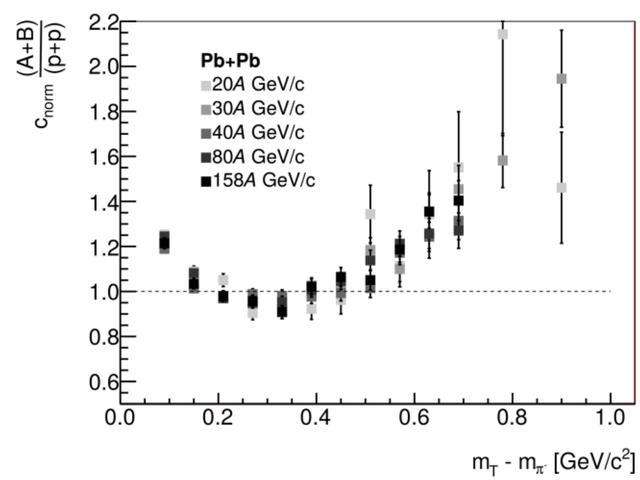


- $m_T$ shape differs significantly between p+p and A+A
  - system size dependence
  - small energy dependence
  - the effect associated to transverse collective flow

# Study of onset of deconfinement: kink

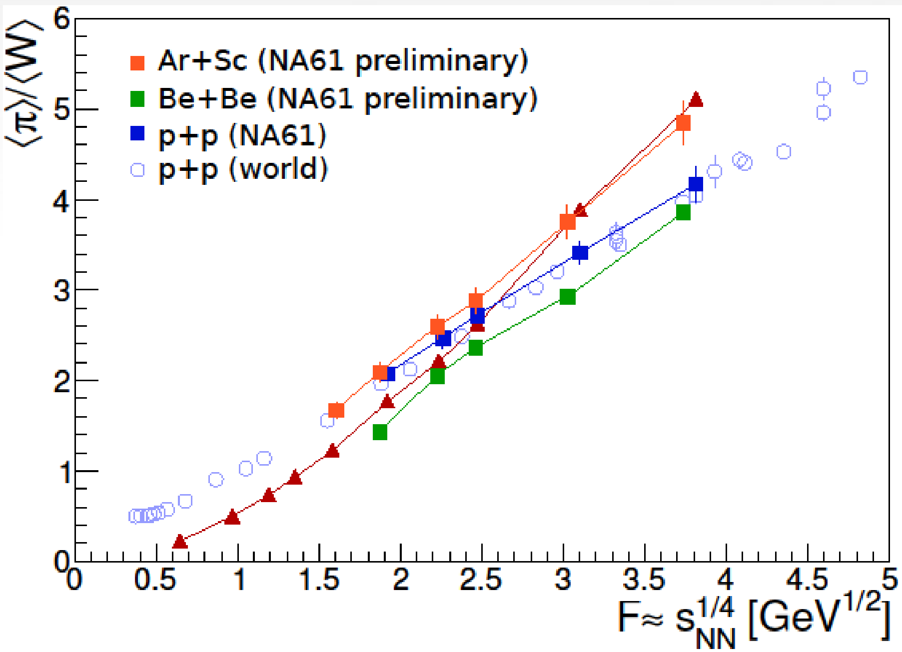


- The slope of energy dependence for heavier systems is larger than for lighter systems at high SPS energies
- Statistical model with phase transition (SMES - Acta Phys. Pol. B30 (1999) 2705) predicts increase of the slope – KINK – of <π>/<W> in QGP due to the larger number of degrees of freedom in comparison to Hadron Gas (HRG)

<π> – mean multiplicity in full acceptance
<W> – mean number of wounded nucleons

# Study of onset of deconfinement: step

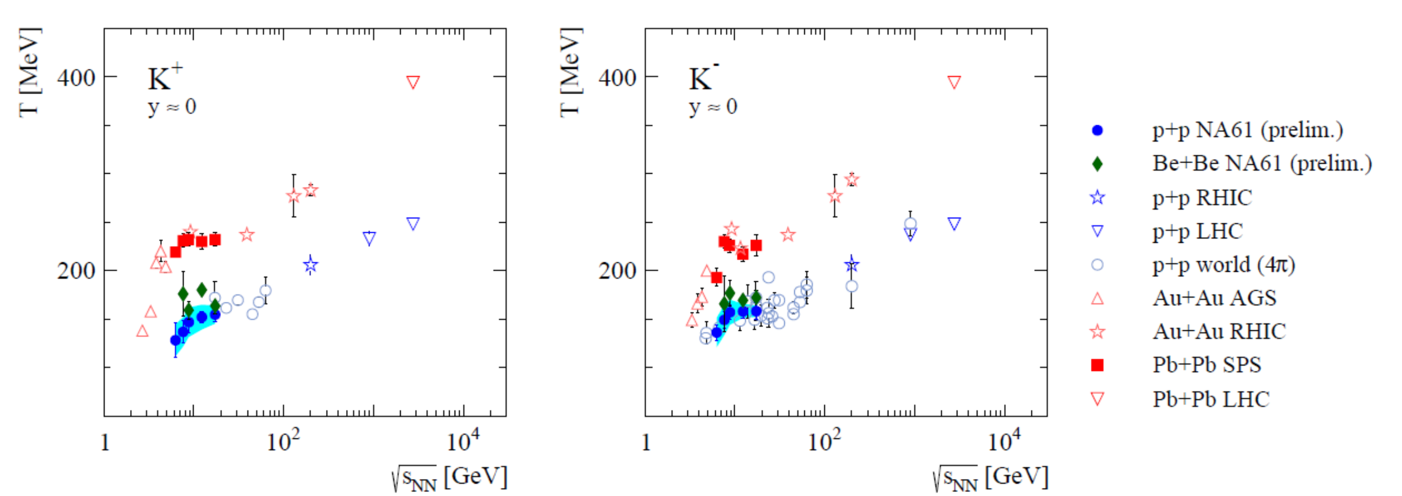


- Plateau – STEP – in the inverse slope parameter of $m_T$ spectra in Pb+Pb collisions observed. It is expected for the onset of deconfinement due to mixed phase of HRG and QGP (SMES)
- Qualitatively similar structure is visible in p+p
- Be+Be is consistent with step structure and slightly above p+p

# Study of onset of deconfinement: horn

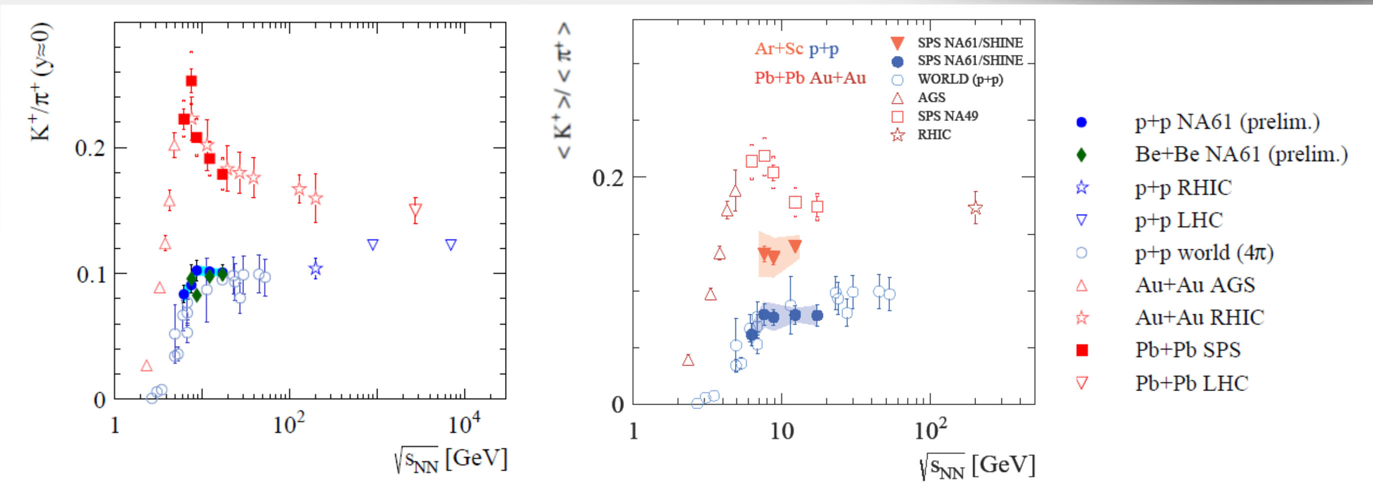


- Rapid changes in $K^+/\pi^+$ – HORN – were observed in Pb+Pb collisions. It was predicted (SMES) as a signature of onset of deconfinement too
- Plateau like structure visible in p+p in mid-rapidity as well as in $4\pi$ acceptance
- Be+Be very close to p+p
- $<K^+>/<\pi^+>$ in Ar+Sc show similar to p+p dependence of the collision Energy and it is placed between p+p and Pb+Pb

# Rapid changes in p+p at SPS – comparison with models

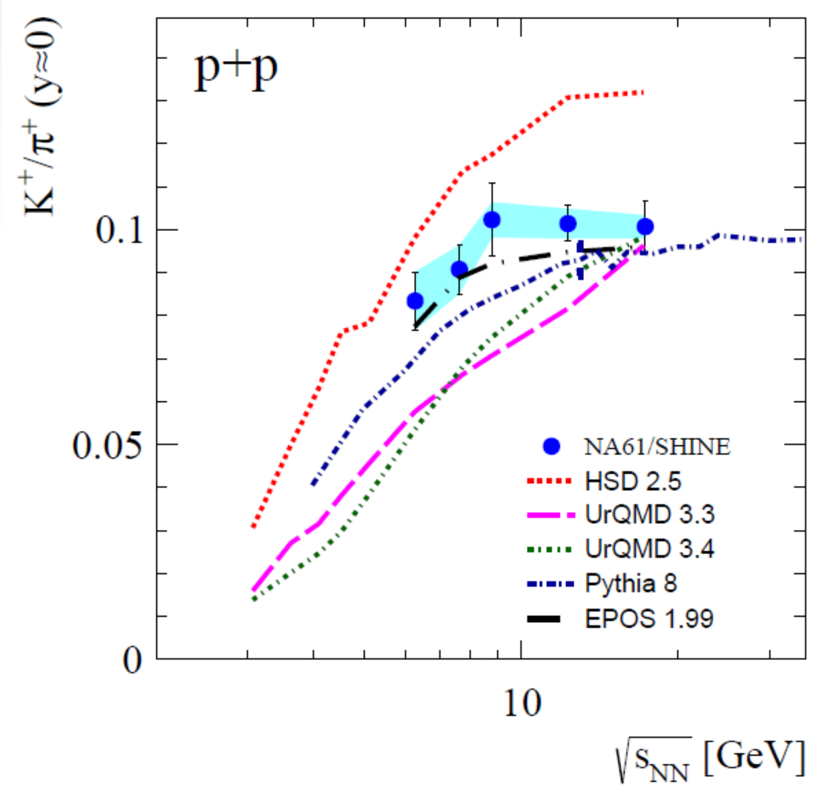


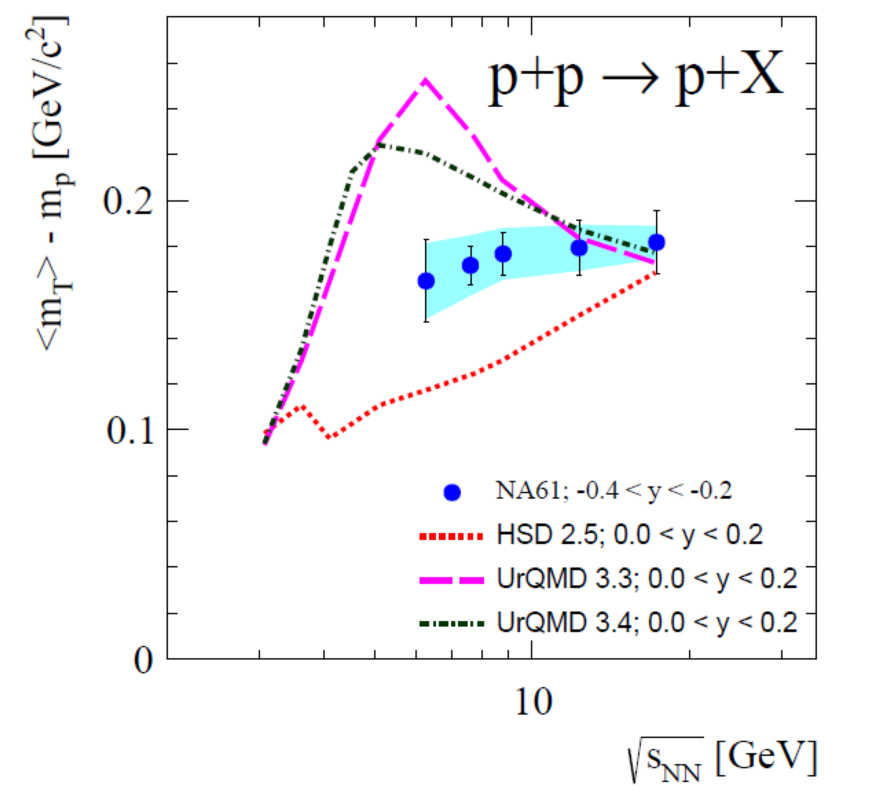


Monte-Carlo models provide poor description of data

# Critical point

# Fluctuations

Theoretical fluctuations in presence of critical point

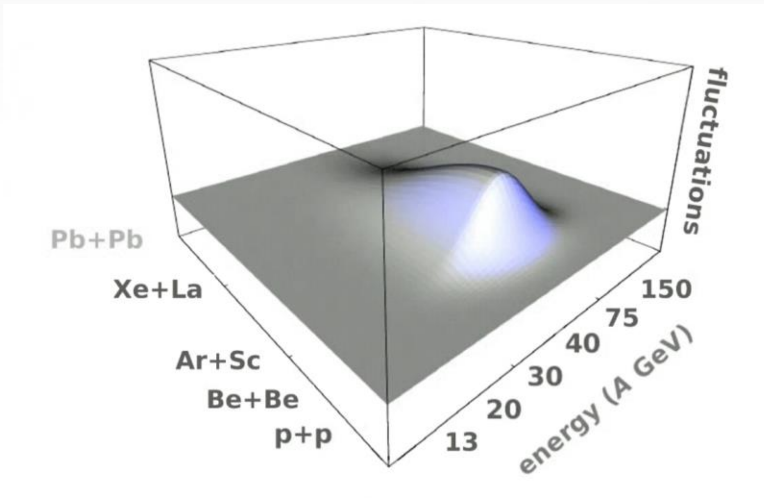


N-$p_T$ fluctuations in p+p and Be+Be, Ar+Sc (central events selected by $E_F$)

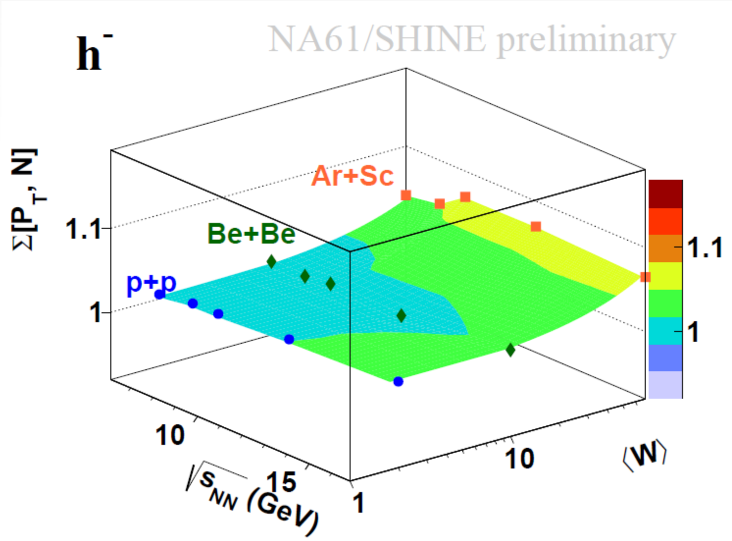


No sign of any anomaly that can be attributed to the critical point (so far)

# Other results

# System size dependence

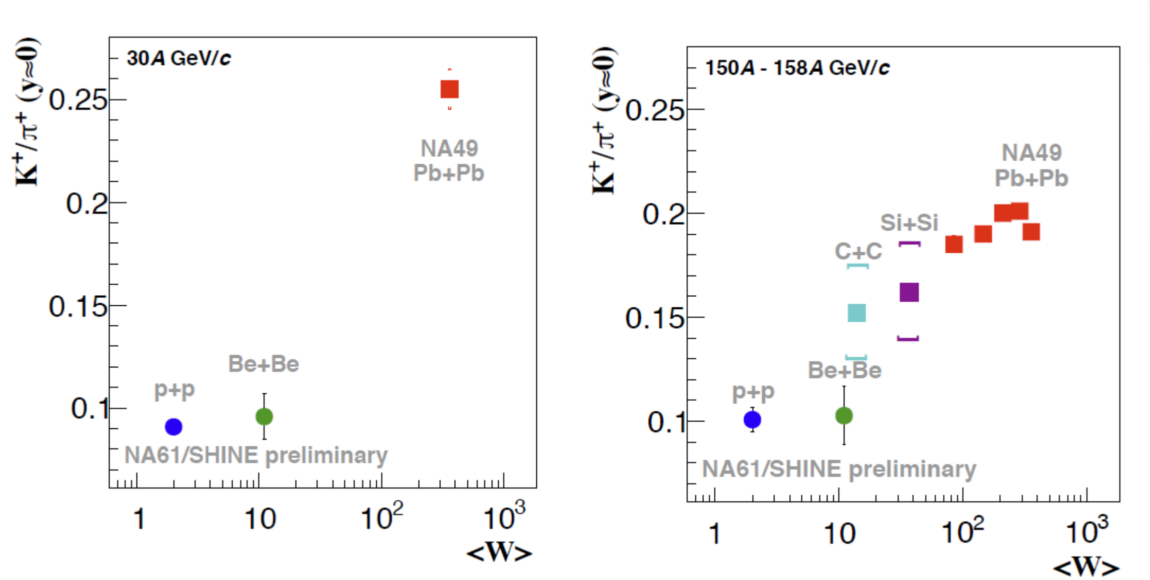


- Surprisingly Be+Be results are very close to p+p independent of collision energy
- Data suggest a jump between light and heavy systems

# System size dependence - multiplicity fluctuations

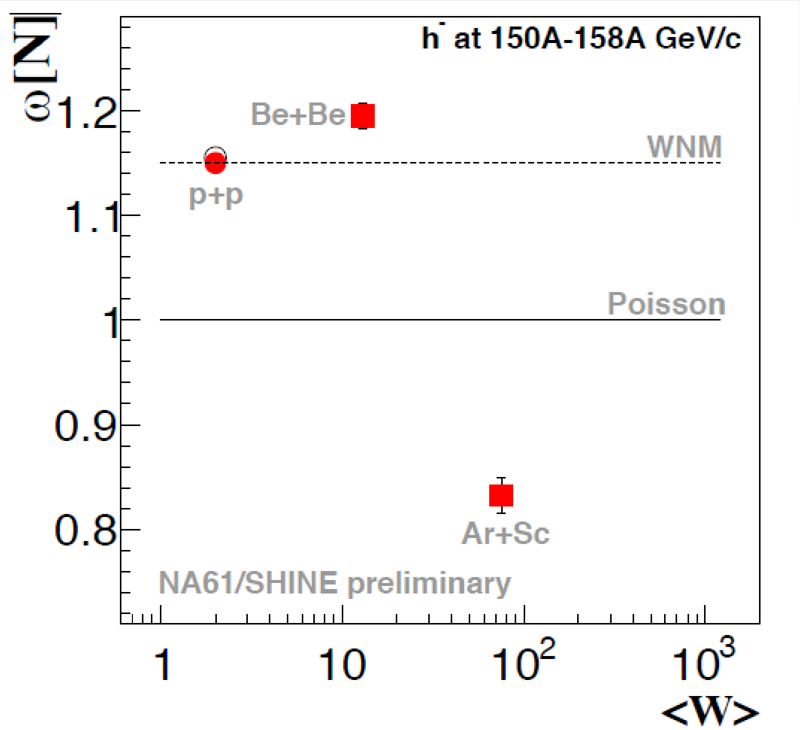


- Why ω[N] in central Be+Be collisions is close to p+p value?
- Why ω[N] is suppressed for central Ar+Sc collisions in comparison to p+p and Be+Be?
- Percolation threshold?

- ω[N] is significantly larger for inelastic p+p interactions and for the central Be+Be collisions than for central Ar+Sc collisions

# Φ(1020) in p+p: rapidity spectra

First measurement of Φ production in p+p interactions at 40 and 80 GeV/c, more detailed and precise measurement at 158 GeV/c

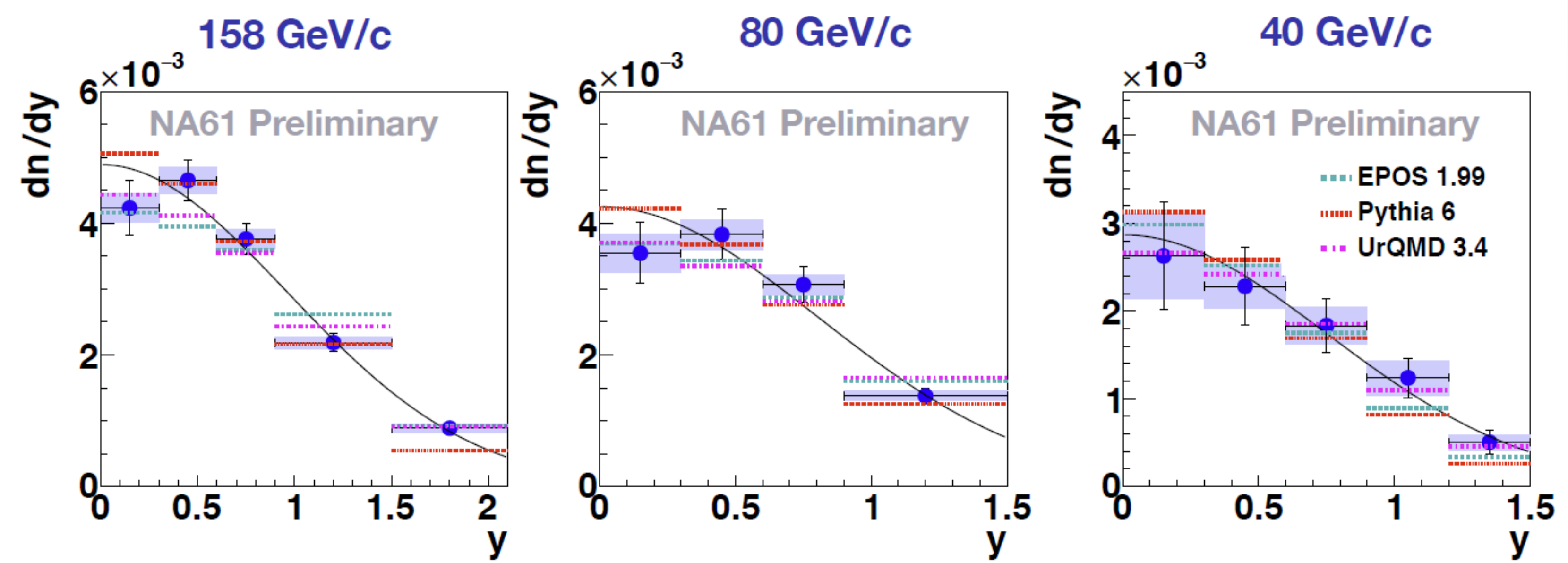


- Large coverage in rapidity, shape approximately described by Gaussian (black curve)
- Models approximately describe spectra shape (models normalised to the integral of data)

# Φ(1020) in p+p: width of rapidity

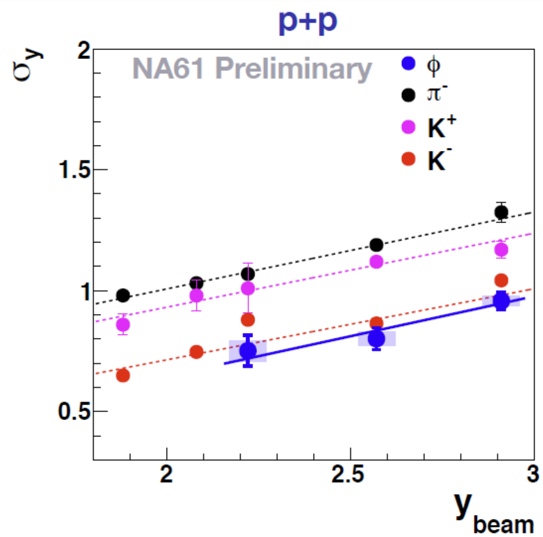


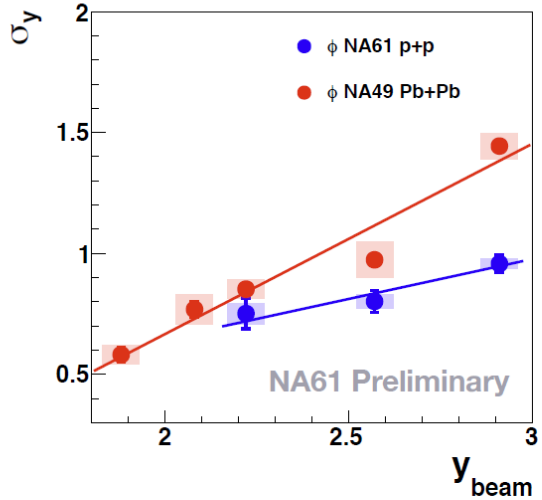


$$\frac{dn}{dy} = \frac{\langle\pi^-\rangle(y_0,\sigma_0)}{2\sigma_0\sqrt{2\pi}} \cdot \left[\exp\left(-\frac{(y-y_0)^2}{2\sigma_0^2}\right) + \exp\left(-\frac{(y+y_0)^2}{2\sigma_0^2}\right)\right]$$

- $\sigma_y$ in p+p follows the trend of other hadrons
- $\sigma_y$ in p+p and Pb+Pb exhibit different $y_{beam}$ dependence

# Φ(1020) in p+p: $\sqrt{s_{NN}}$ dependence

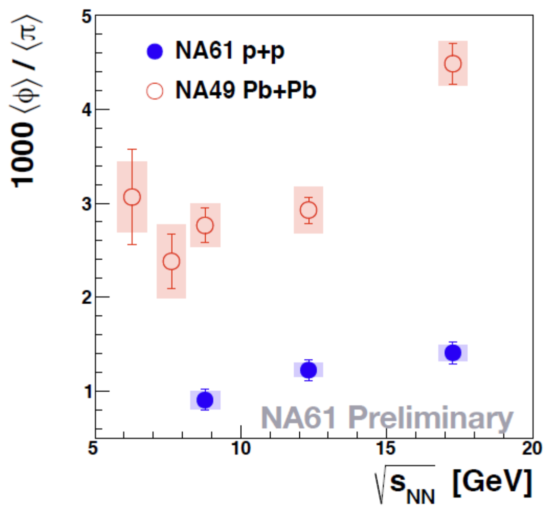


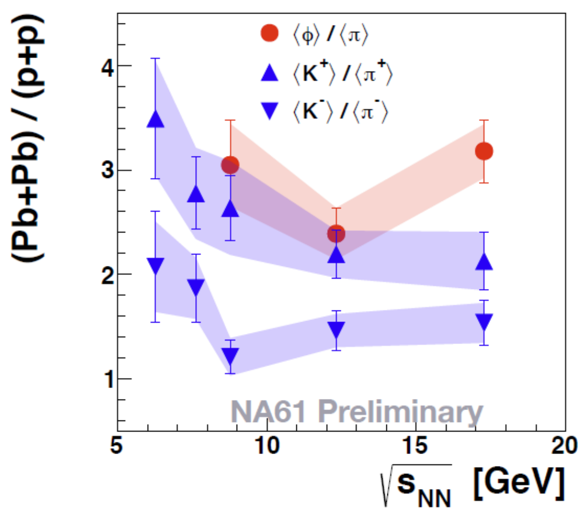


- <Φ>/<π> in p+p increases with $\sqrt{s_{NN}}$
- <Φ>/<π> ratio about 3x larger in Pb+Pb collisions independently of interaction energy
- Enhancement of <Φ>/<π> ratio is close to $<K^+>/<\pi^+>$, larger than for $<K^->/<\pi^->$

# Λ in p+p: <Λ>

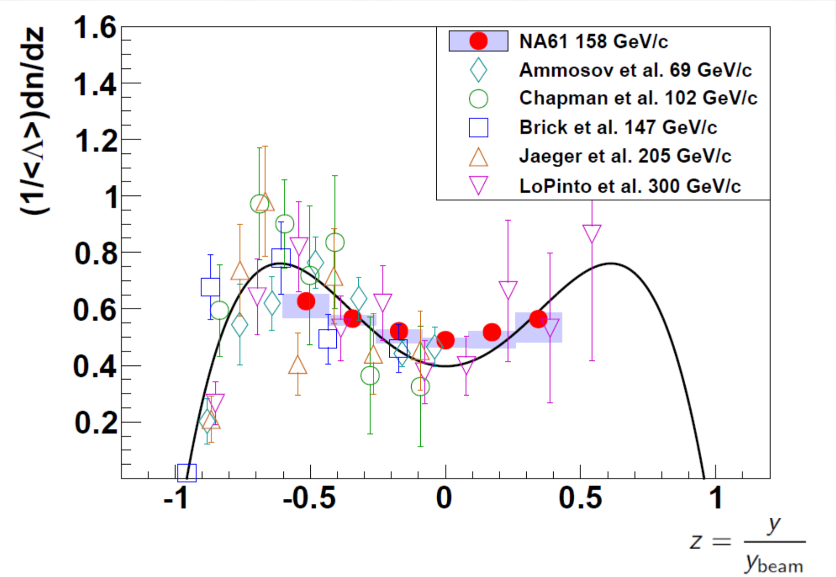


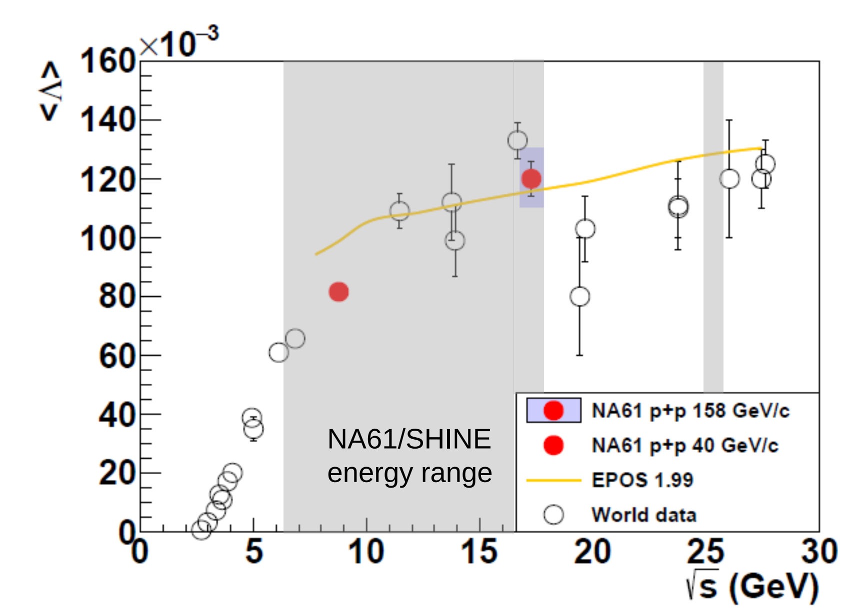


- The NA61 data follow the trend set by the world data, at the same time reducing the uncertainty significantly
- EPOS overestimates <Λ> at 40 GeV/c

# <Λ> / <π>

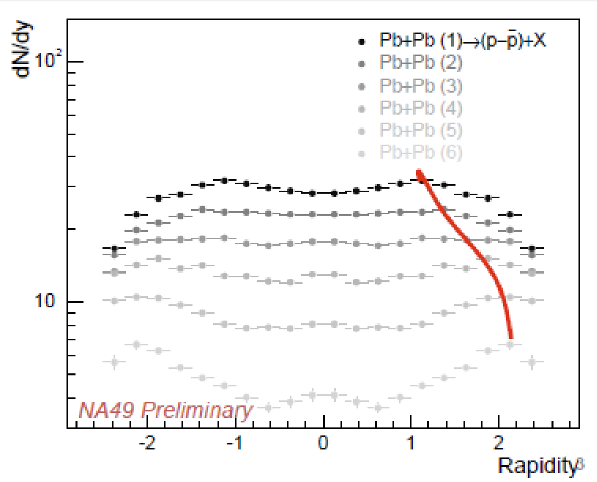


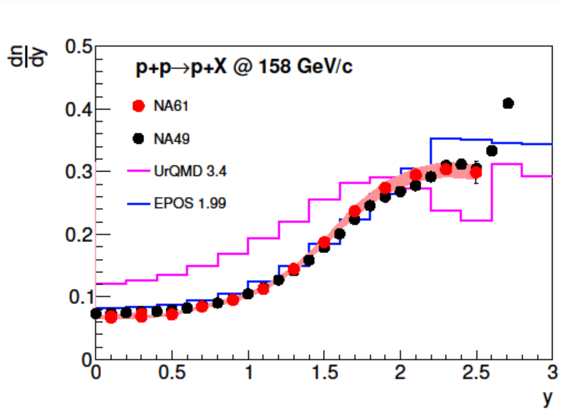


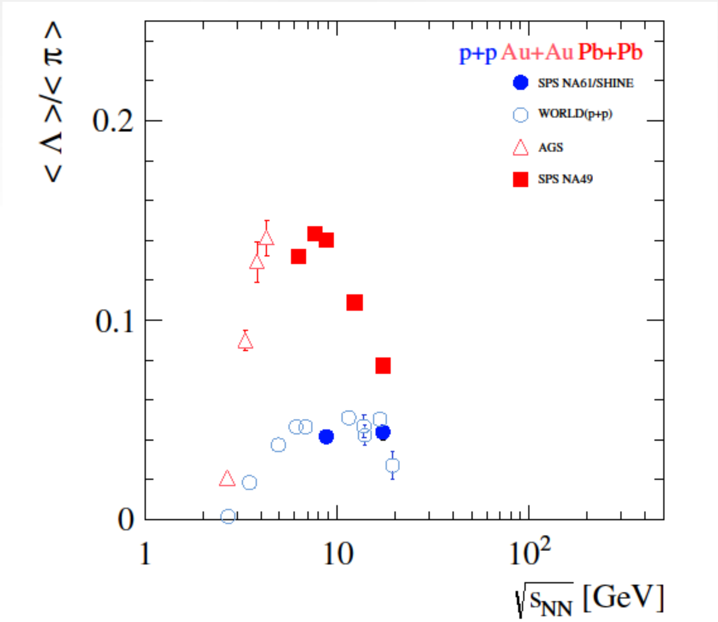


- The presented NA61/SHINE results agree with the world data
- Measurements in A+A collisions at the AGS and by NA49 show a different behavior than that observed in p+p reactions due to difference in baryon density

# Interaction cross-section of $^{7}$Be on $^{9}$Be

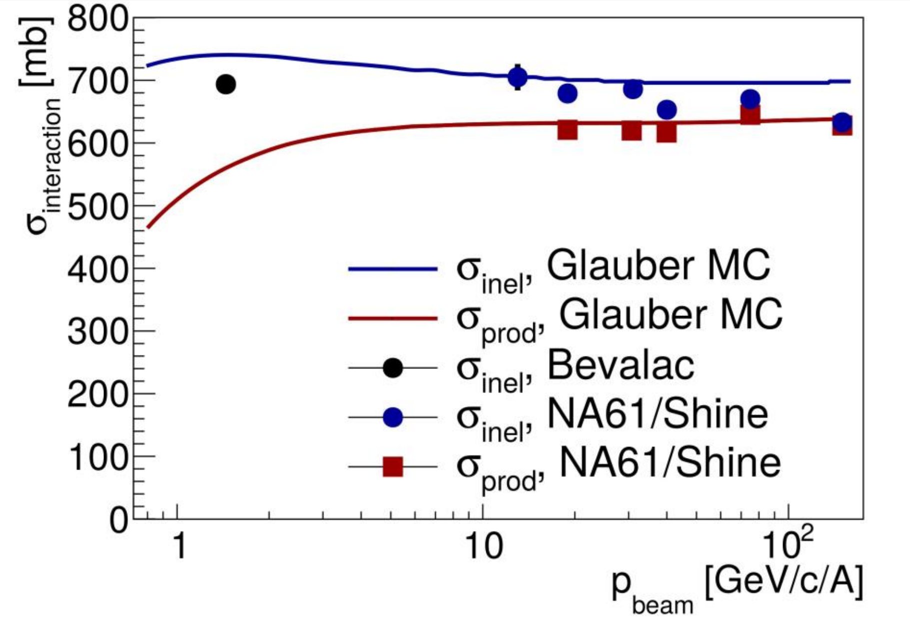


$$\sigma_{tot} = \sigma_{inel} + \sigma_{el}$$
$$\sigma_{inel} = \sigma_{prod} + \sigma_{qe}$$

- *inelastic cross section* - initial state particles are different than final state ones
- *elastic cross section* - initial and final state particles are the same
- *quasi–elastic cross section* – either target or projectile fragmented, but no new particles
- *production cross section* - there is at least one new particle in the final state

- Values measured by NA61/SHINE are in good agreement with earlier measurement at lower momentum [Tanihata et al., PRL 55, 2676, 1985], as well as with predictions of the Glauber - based Glissando model [Broniowski, Rybczyński, Bozek, Comput. Phys. Commun. 180, 69, 2009]
- NA61 measurements together with ~1*A* GeV/c Bevalac data established energy dependence of the inelastic cross section

# Neutrino and cosmic ray program

# Data taking plan

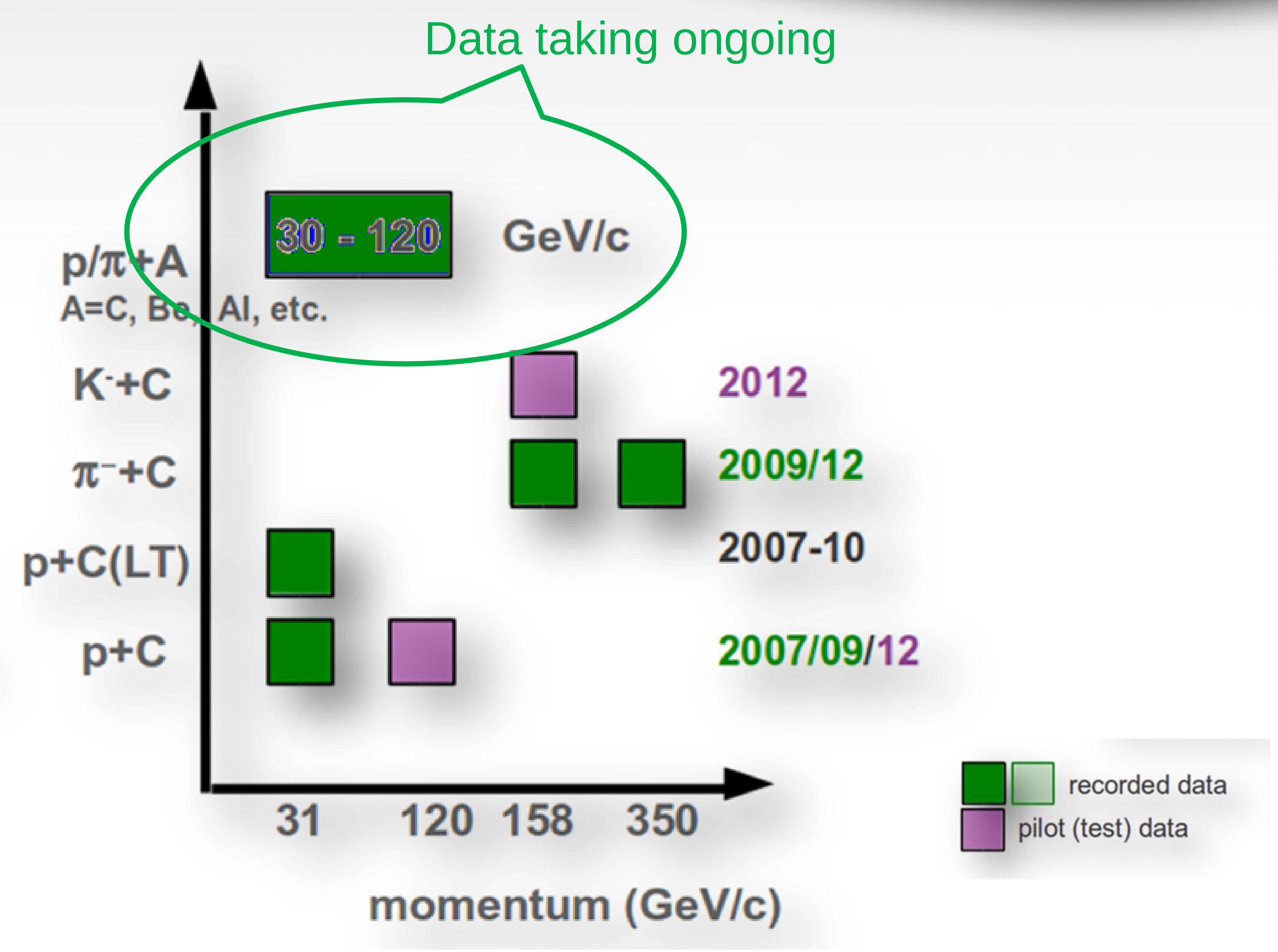

# Hadron-production measurements for neutrino experiments

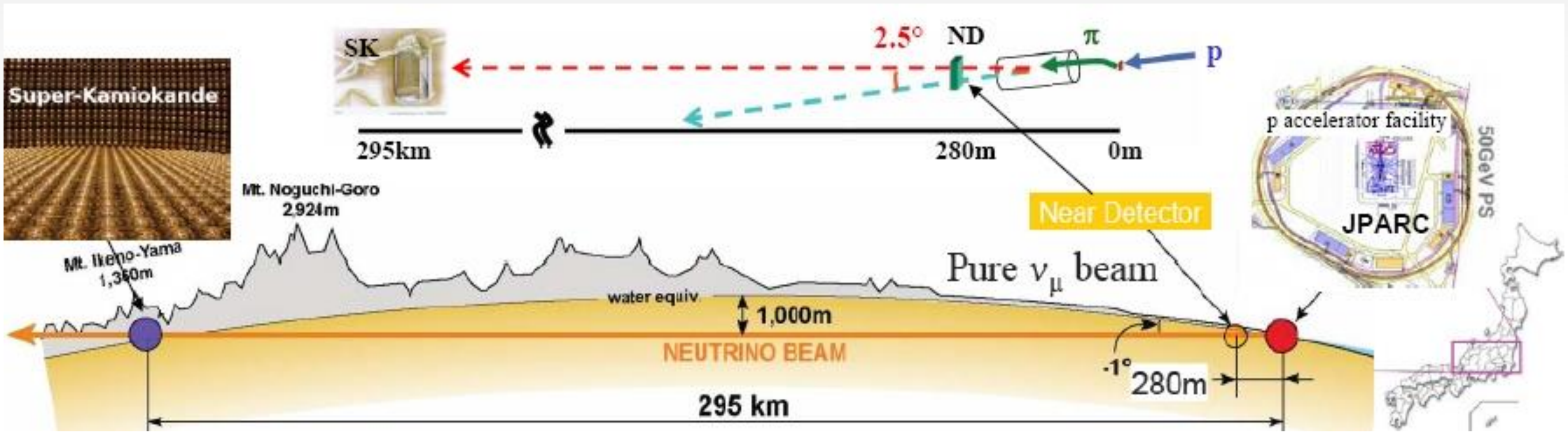


The T2K experiment published a measurement of $\theta_{13}$ angle in the neutrino mixing matrix (PRL 107, 041801 (2011))

Systematic error estimate was based on the NA61/SHINE results

# Hadron-production measurements for neutrino experiments

## NA61/SHINE 2009 p+C @ 31 GeV

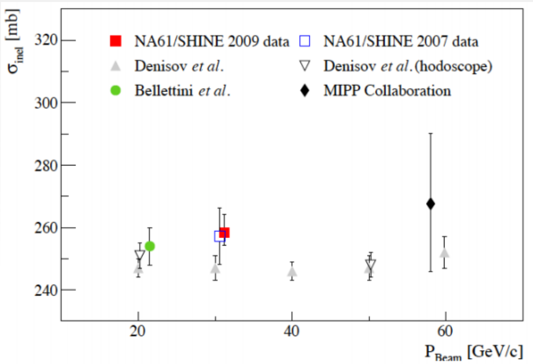


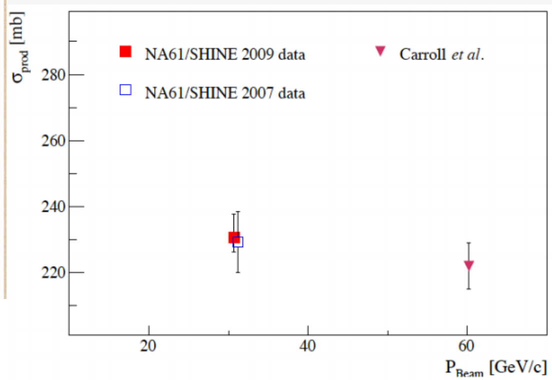


$\sigma_{\mathrm{inel}} = 258.4 \pm 2.8(\mathrm{stat}) \pm 1.2(\mathrm{det})^{+5.0}_{-2.9}(\mathrm{mod})\,\mathrm{mb}$ $\sigma_{\mathrm{prod}} = 230.7 \pm 2.8(\mathrm{stat}) \pm 1.2(\mathrm{det})^{+6.3}_{-3.5}(\mathrm{mod})\,\mathrm{mb}$

Eur.Phys.J. C76 (2016) no.2, 84

## Hadron Production: p+T2K replica—>π+X

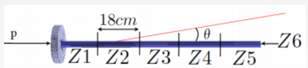


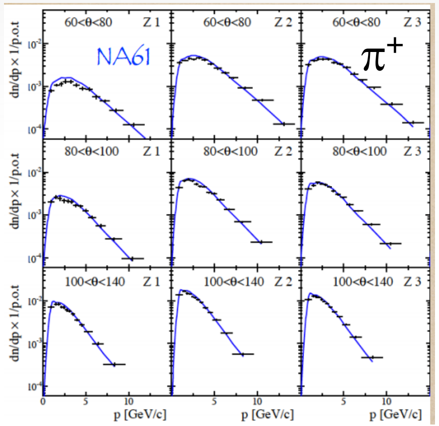


Eur.Phys.J. C76 (2016) no.11, 617

## T2K Flux Uncertainty with new NA61 data

### With NA61 p+C thin target result

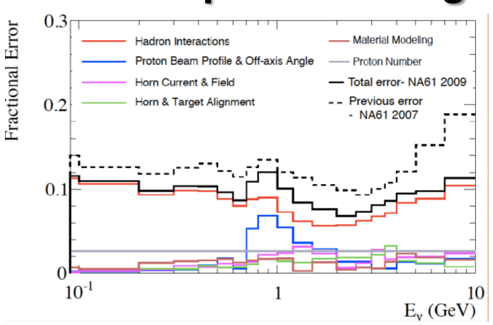


T2K ν-flux uncertainty improves ~25% compared to previous result

Can reduce pion production contribution to the flux error to 4%

### With NA61 p+T2K replica target result

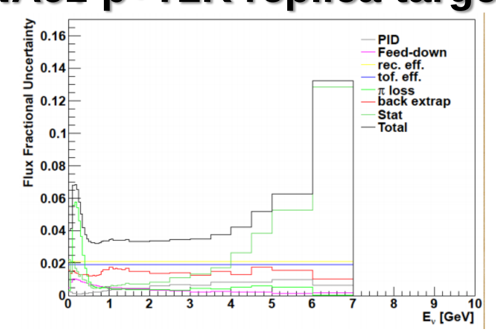

# Hadron-production measurements for cosmic ray experiments

Cosmic ray composition of central importance for understanding sources, kink, ankle...

Modern detector installations: high statistics/quality data

Indirect measurement (extensive air showers): simulations needed

Strong model dependence: due mainly to simulation of m production

m production related to hadronic interactions at fixed-target energies

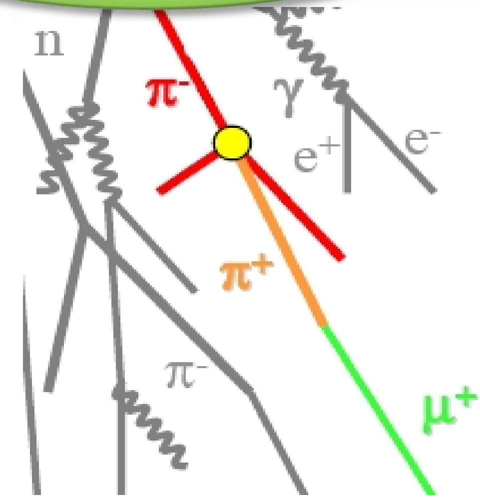

# Hadron-production measurements for cosmic ray experiments

## Spectra - example

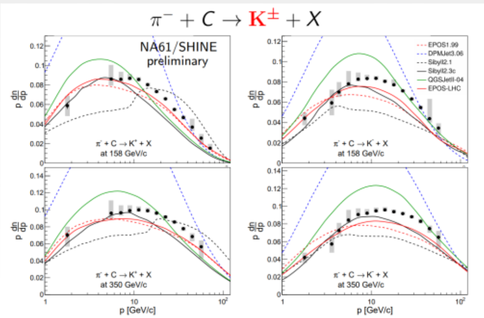


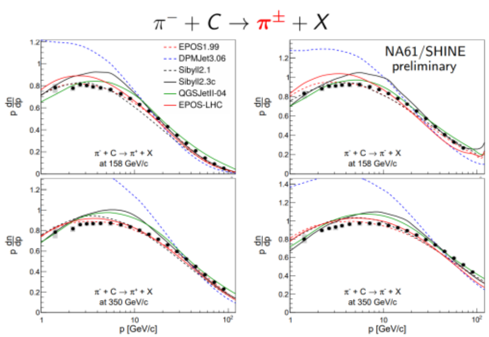


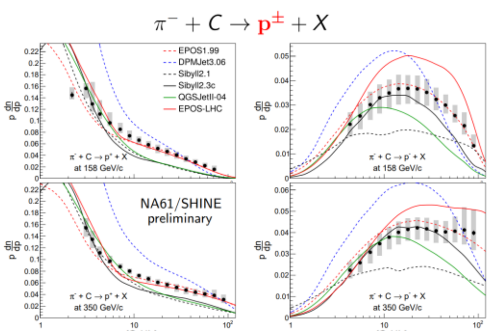


## Cross sections measurements

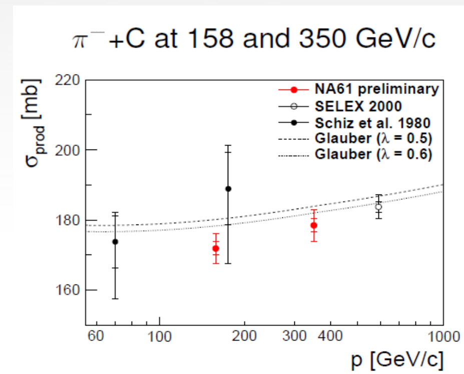


## Input for validation/tuning of Monte Carlo generators

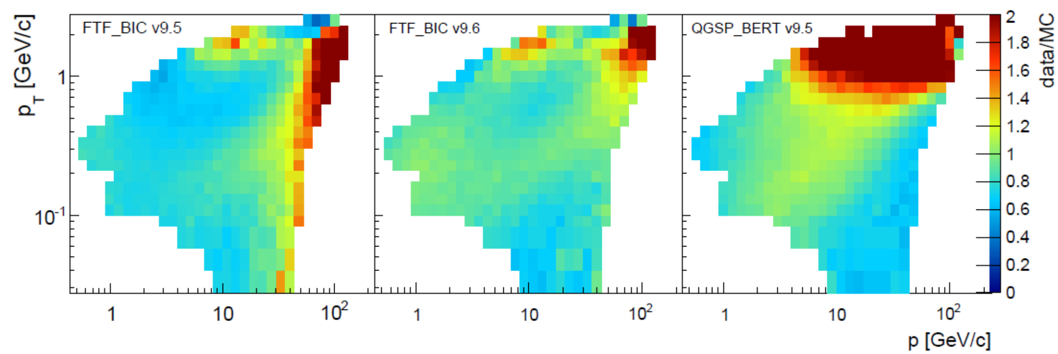

# Future of NA61/SHINE

# Open charm measurements

D$^0$ candidates selected by TPCs only

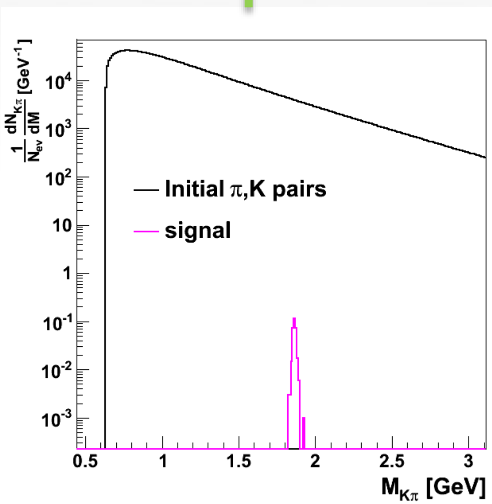


- Feasibility of the D$^0$ meson measurements in two body decay channel: D$^0$ → K$^+$ + $\pi^-$, in central Pb+Pb collisions at the SPS energy range

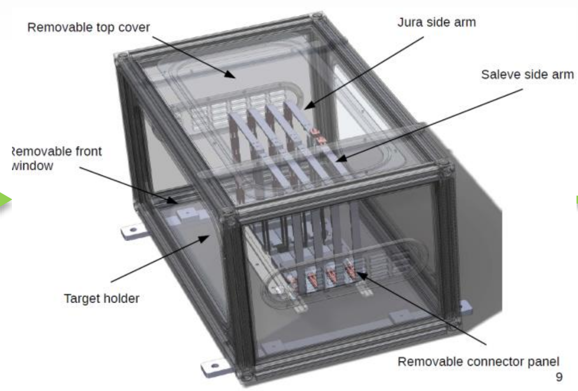


D$^0$ candidates selected by TPCs and vertex detector

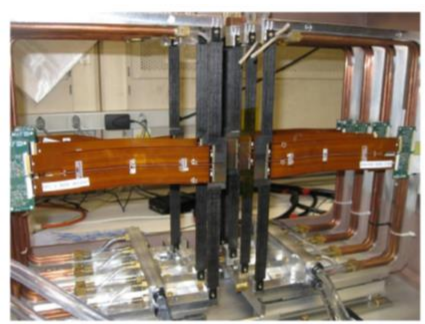

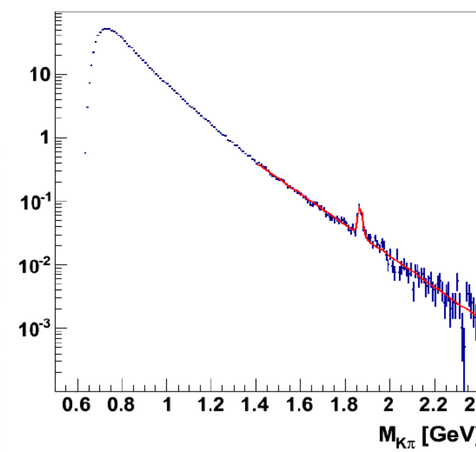


- Vertex detector:
  - Small Acceptance Vertex Detector was commissioned in 2015
  - Pilot data was recorded in 2016
  - Vertex fit resolution on the level of 50 μm
  - four pixel detection stations
  - MIMOSA-26AHR sensor

# NA61/SHINE in 2021–2024

Detector upgrades during Long Shutdown in 2019–2020: 1 kHz readout by upgrading TPCs readout electronics, Large Acceptance Vertex Detector, increase and improve beam intensity and quality, ToF, PSD

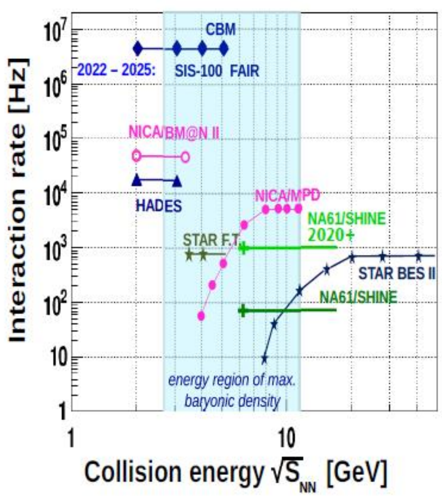


10 days in 2018

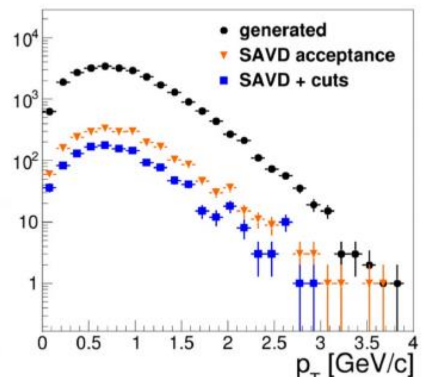


≈ 3000 $D^0$ in 4 M events

10 days in 2021
(1000Hz + LAVD)

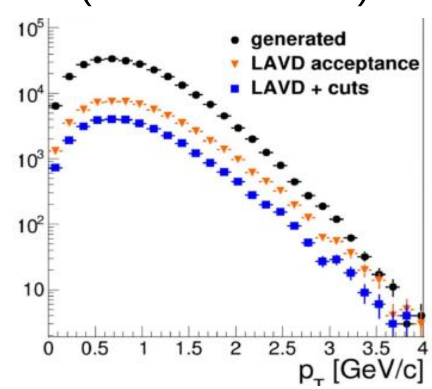


≈ 40000 $D^0$ in 40 M events

# NA61/SHINE plans

- Measurements of Xe+La collisions at 20A – 150A GeV/c in 2017
- Measurement of Pb+Pb collisions at 150A GeV/c in 2018
  - New Vertex detector ⟶ pilot open charm measurements and precise measurement of fluctuations and collective effects in Pb+Pb collisions
- Detector upgrade foreseen during long shutdown (2019-2020)
- NA61/SHINE in 2021-2024: High statistics beam momentum scan with Pb+Pb collisions for the precise measurements of open charm and multi-strange hyperon production
- NA61/SHINE performs precise particle production for neutrino physics programs which is planned to be continued after 2020
- NA61/SHINE plans to measure fragments production and energy dependence cross section for AMS experiment after 2020

# Summary

# Summary

NA61/SHINE performs the unique system size vs energy scan for systematic study of the phase diagram of strongly interacting matter

- p+p, Be+Be and Ar+Sc data collected and being analysed
- Unexpected system size dependence of K+/ π+ ratio observed in p+p and Be+Be
- Plans to extend NA61/SHINE program with measurements of open charm and multi-strange hyperon production in 2021-2024

# The Collaboration

National Nuclear Research Center, Azerbaijan
Faculty of Physics, University of Sofia, Bulgaria
Ruder Boskovic Institute, Croatia
LPNHE, University of Paris VI and VII, France
Karlsruhe Institute of Technology, Germany
Fachhochschule Frankfurt, Germany
Institut für Kernphysik, Goethe-Universität, Germany
Nuclear and Particle Physics Division, University of Athens, Greece
Wigner RCP, Hungary
Institute for Particle and Nuclear Studies (KEK), Japan
University of Bergen, Norway
Jan Kochanowski University in Kielce, Poland
National Center for Nuclear Research, Poland
Institute of Physics, Jagiellonian University, Poland
AGH-University of Science and Technology, Poland
Institute of Physics, University of Silesia, Poland
Faculty of Physics, University of Warsaw, Poland
Department of Physics and Astronomy, University of Wroclaw, Poland
Faculty of Physics, Warsaw University of Technology, Poland
IFJ PAN, Poland
Institute for Nuclear Research, Russia
Joint Institute for Nuclear Research, Russia
St. Petersburg State University, Russia
National Research Nuclear University MEPhI, Russia
University of Belgrade, Serbia
ETH Zürich, Switzerland
University of Bern, Switzerland
University of Geneva, Switzerland
University of Colorado Boulder, USA
Los Alamos National Laboratory, USA
Department of Physics and Astronomy, University of Pittsburgh, USA
Fermilab, Neutrino Division, USA

seweryn.kowalski@us.edu.pl

# THANK YOU

# BACKUP SLIDES

# Secondary beryllium beam

- Fragmentation target length optimized to maximize the production of the desired fragment
- Double magnetic spectrometer separates fragments according to the selected magnetic rigidity
- Possible to use degrader, Cu plate where ions lose energy according to the charge

Secondary beam

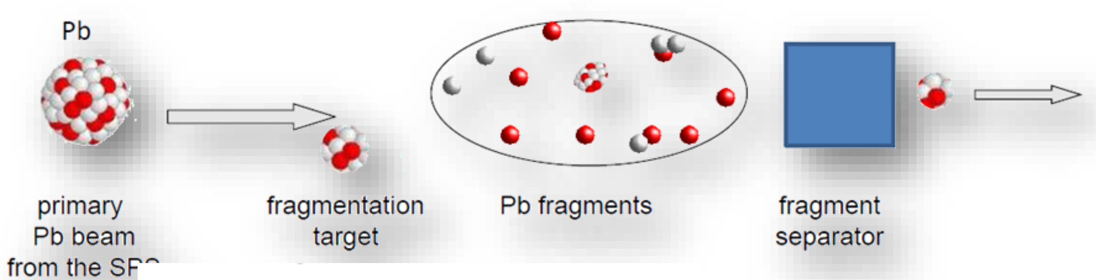


CERN COURIER

Apr 27, 2012

**Light work with heavy ions**

H. Stroebele & I. Efthymiopoulos

# NA61/SHINE Detector

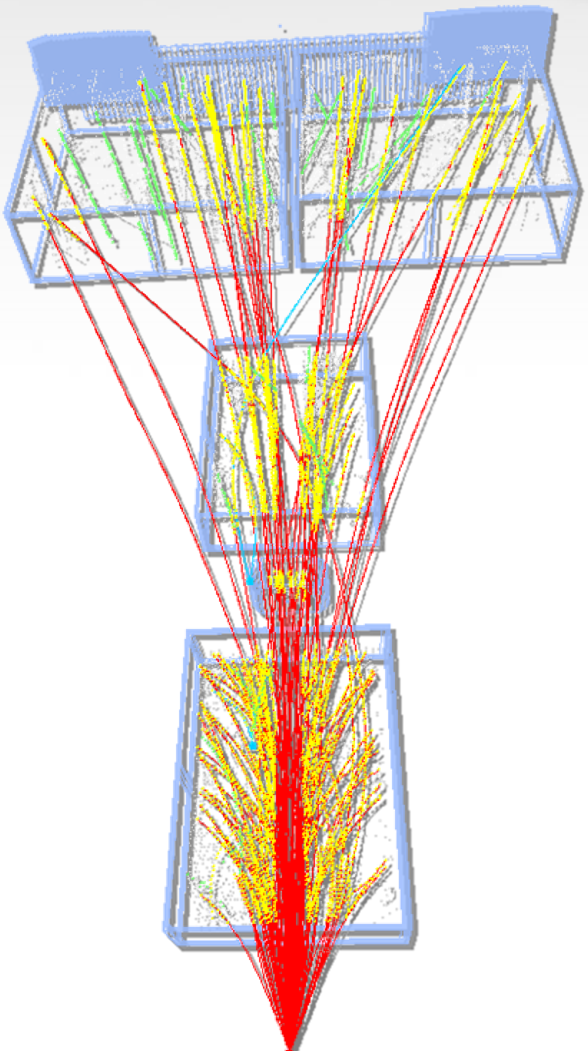

$^7$Be+$^9$Be@158A GeV/c

- Large acceptance: 50%
- High momentum resolution:
  - $\sigma(p)/p^2 \approx 10^{-4}$ (GeV /c)$^{-1}$ (at full B=9 T m)
- ToF walls resolution:
  - ToF-L/R: $\sigma(t) \approx$ 60ps; ToF-F: $\sigma$ (t) $\approx$ 120ps
- Good particle identification:
  - $\sigma(dE/dx)/ < dE/dx > \approx 0.04$; $\sigma(m_{inv}) \approx$ 5MeV
- High detector efficiency: 95%
- Event recording rate: 70 events/sec

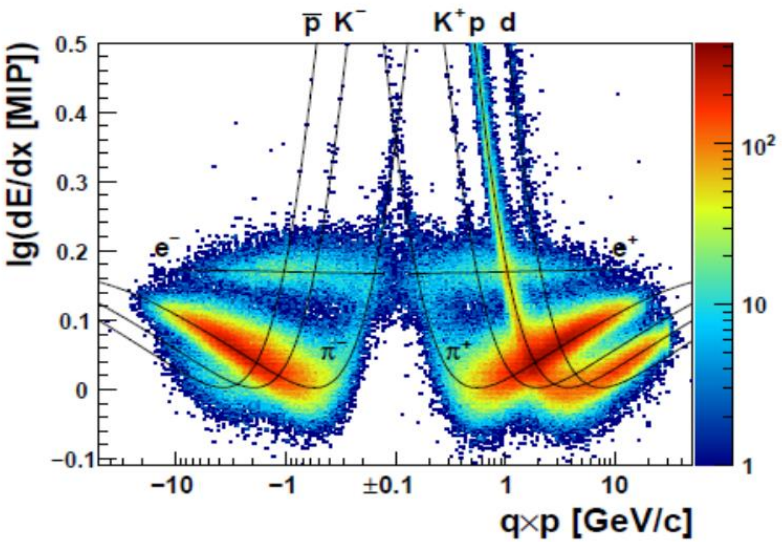

# Energy loss (dE/dx) method

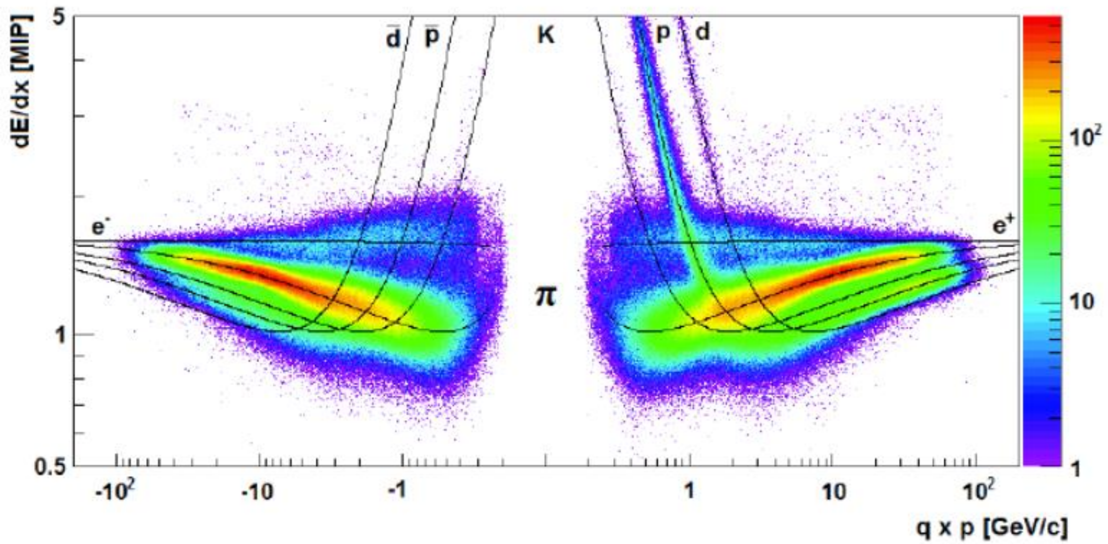


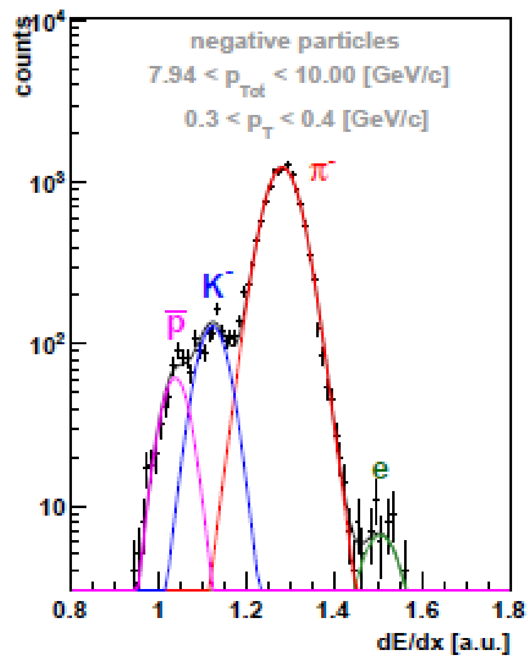


- In each p, $p_T$ bin sum of Gauss functions is fitted to the dE/dx spectrum
- For each track the probability for being a hadron of specific type is calculated based on the fitted dE/dx distribution
- Sum of these probabilities gives the mean multiplicity of the identified hadrons

# Energy loss (dE/dx) vs time of flight (tof) method

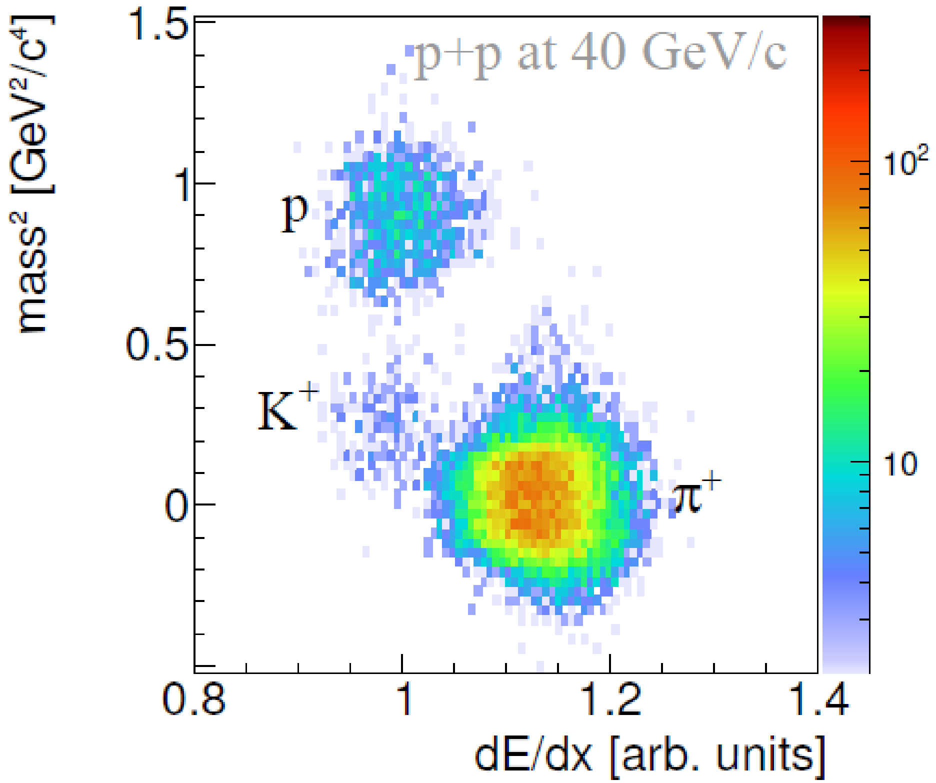


- Fit a two-dimensional weighted Gaussian function in the mass$^2$ vs dE/dx plane

# $V^0$ – method

- Method example
  - Decay channel: $\Lambda \rightarrow p + \pi^-$
  - Invariant mass histograms in $p_T$ and y bins
  - In each p, $p_T$ bin sum of signal (i.e. Lorentzian) and background functions is fitted to the invariant mass spectrum

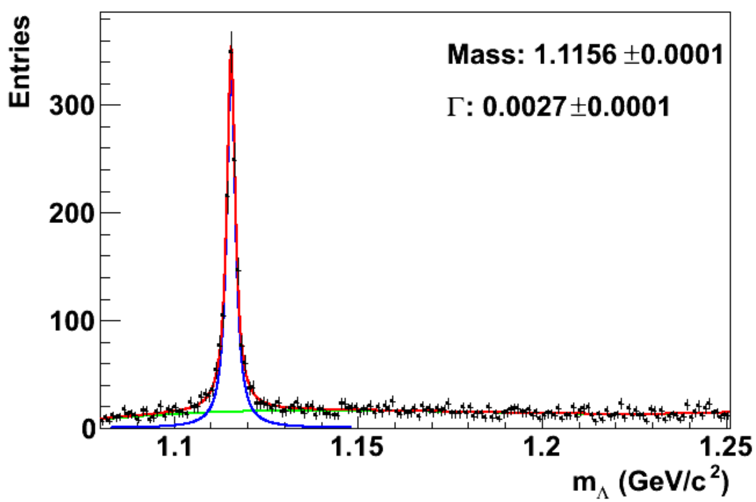


$\Lambda$ mass from PDG 1115.678±0.006±0.006 GeV/$c^2$

Lifetime is calculated based on the difference between position of the main and the decay vertex

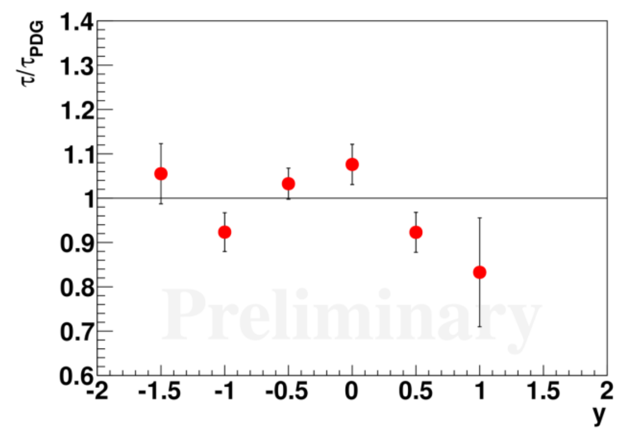


Results are consistent with PDG value ($c\tau_\Lambda$ = 7.89 cm)

# Precise measurements ($\pi^-$ meson)

p+p collisions

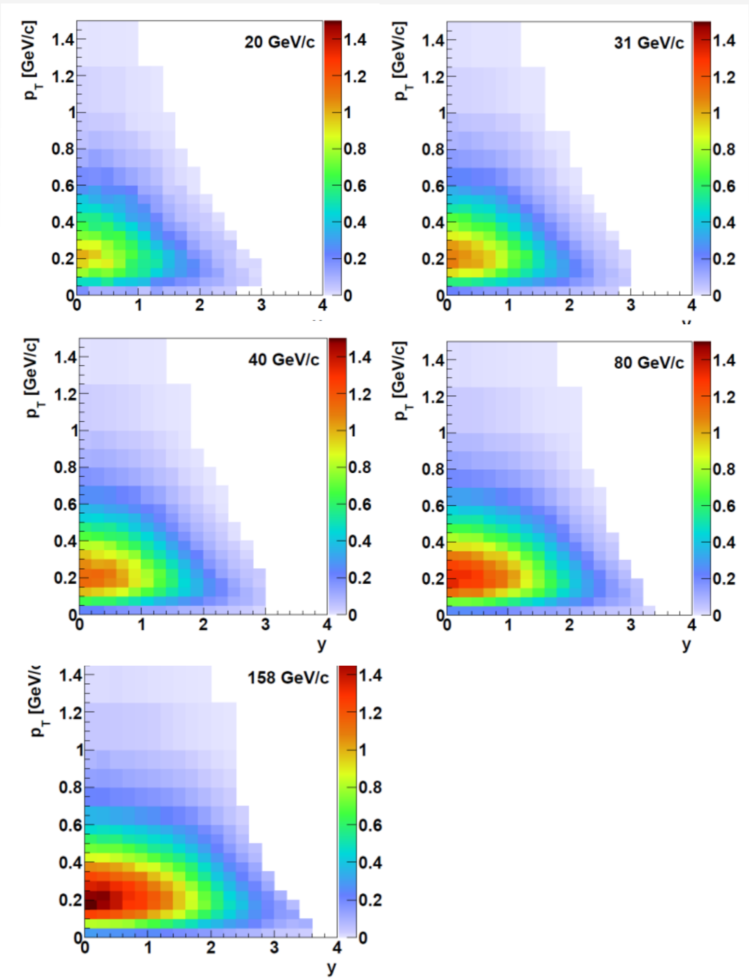


$^{7}$Be+$^{9}$Be collisions

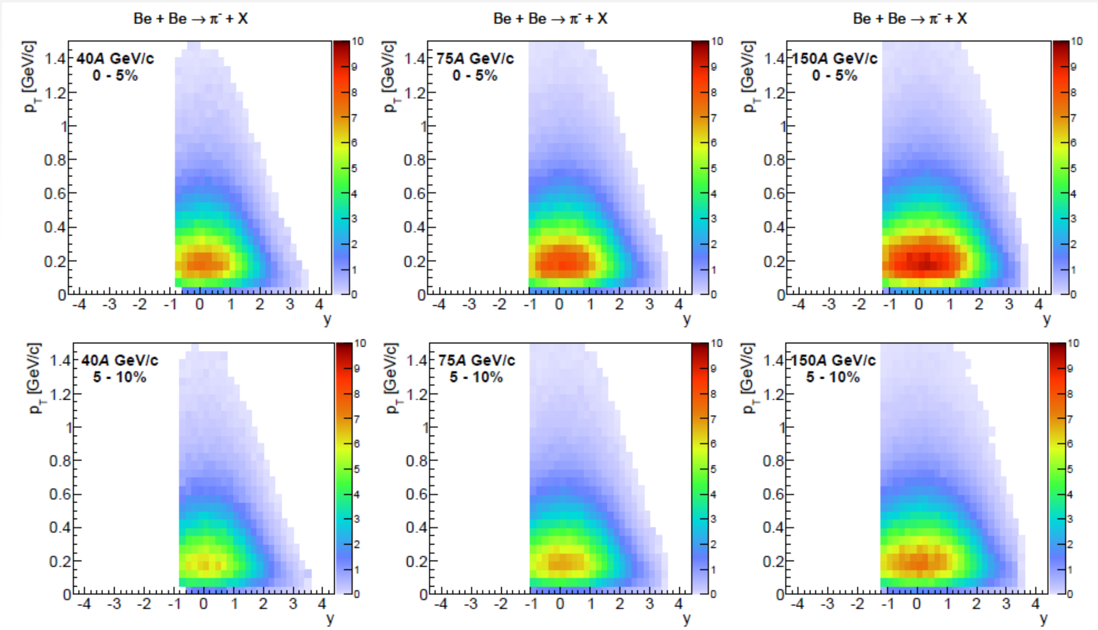

# Λ in p+p at 40 GeV/c

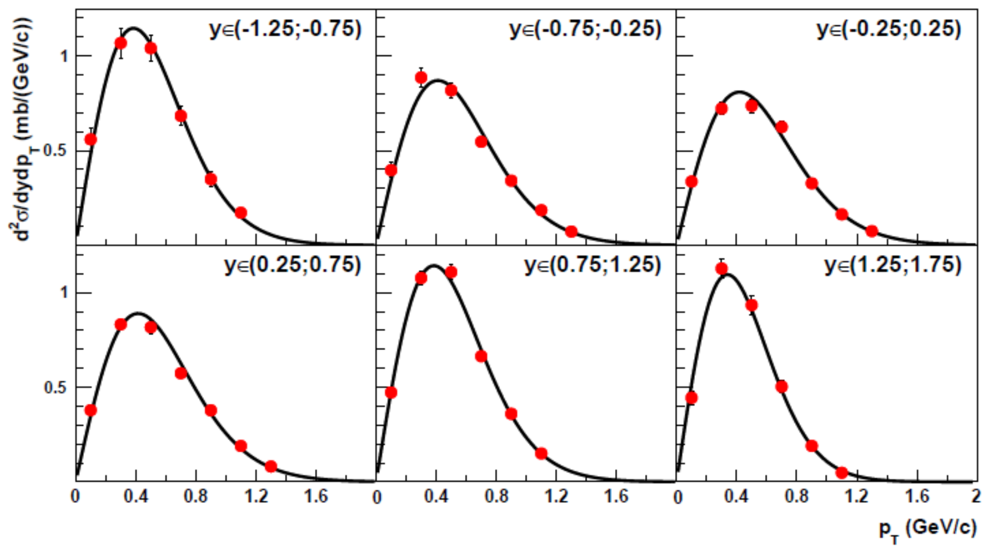


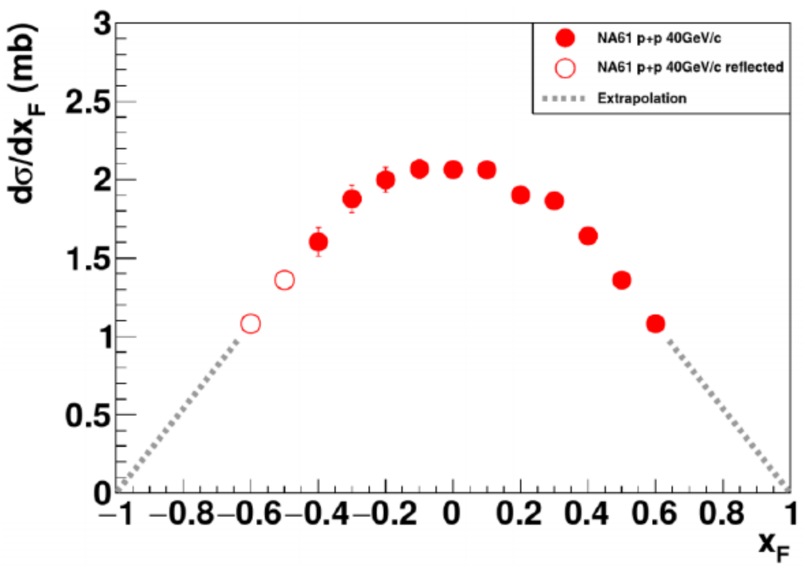


Solid lines: exponential fit.

Dotted lines: used to extrapolate to 4π

# Rapidity distributions

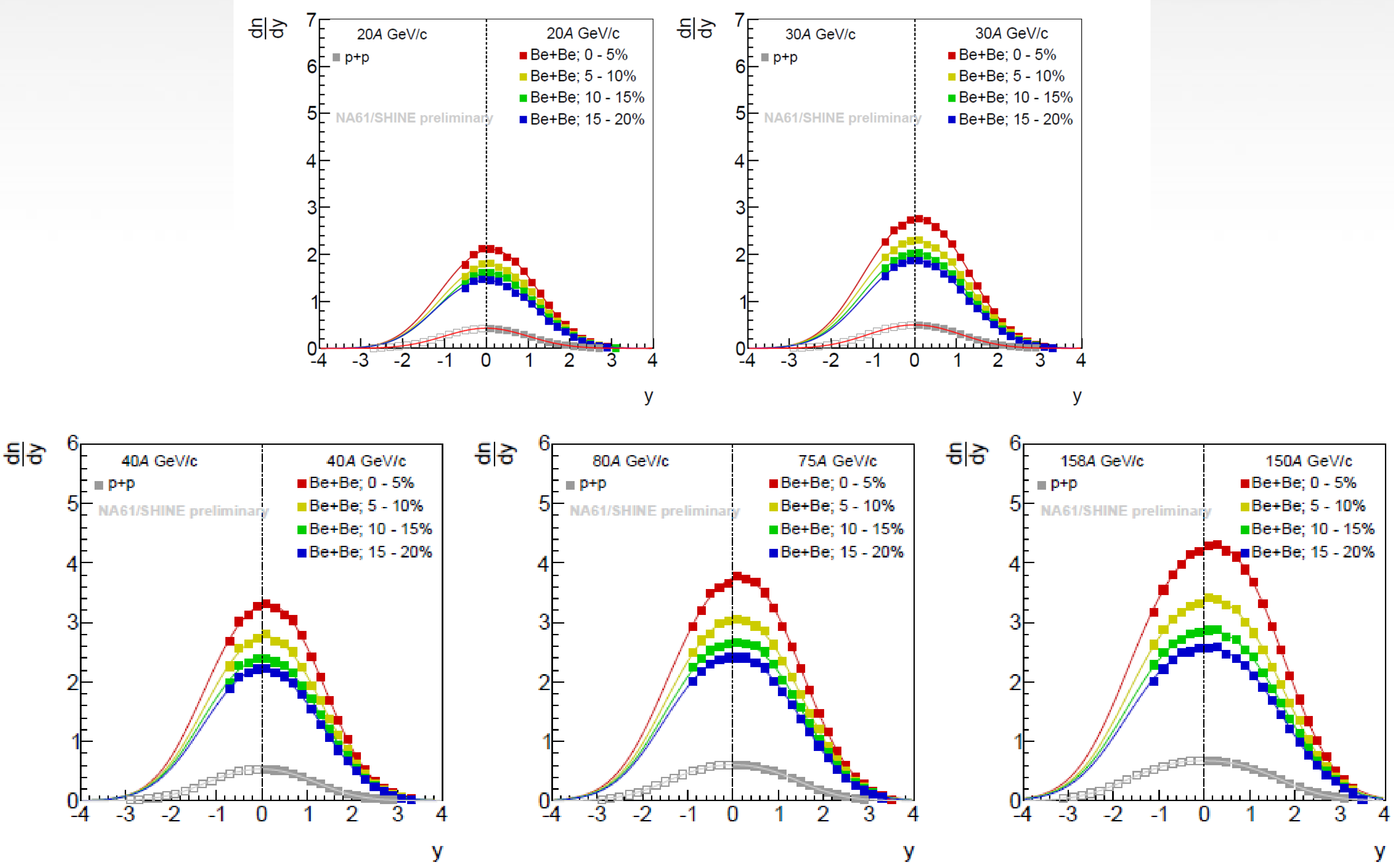

# $h^-$ analysis method

- Majority (more than 90%) of negatively charged particles are $\pi^-$ mesons
- The small contribution of other particles ($K^-$, $\bar{p}$, and decays from $\Lambda$ and $K^0_S$) is subtracted based on data and model predictions

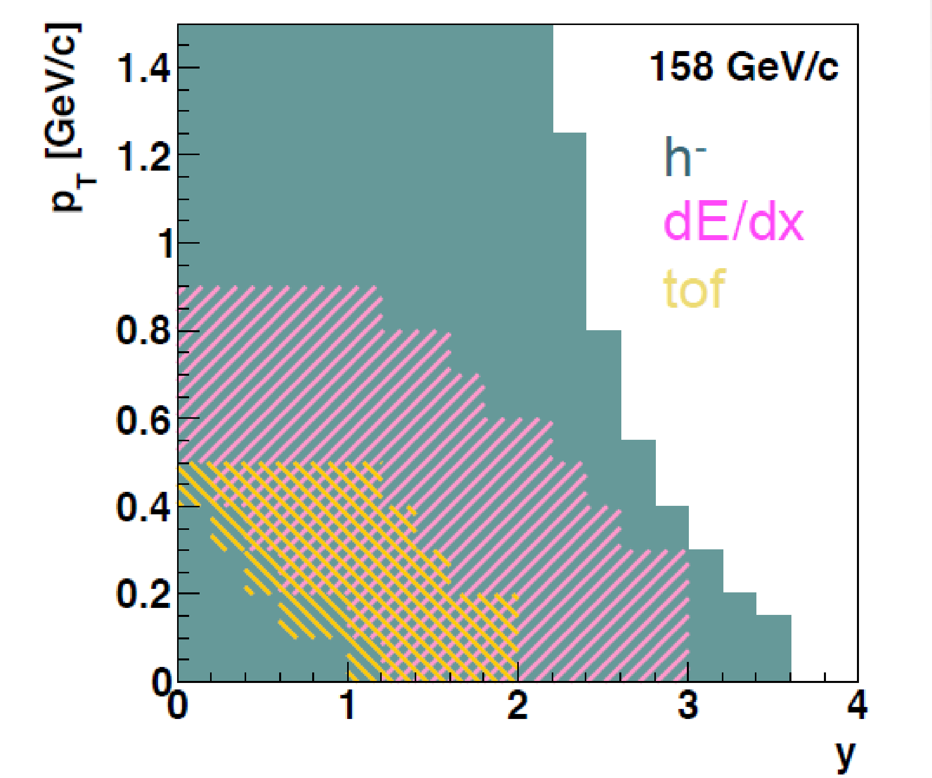

# Centrality selection in ion collisions

- PSD (Projectile Spectator Detector) is located on the beam axis and measures the forward energy $E_F$ related to the non-interacting nucleons of the beam nucleus
- Cuts on $E_F$ allows to select different centrality classes
- Four event classes

0 - 5% 5 - 10% 10 - 15% 15 - 25%

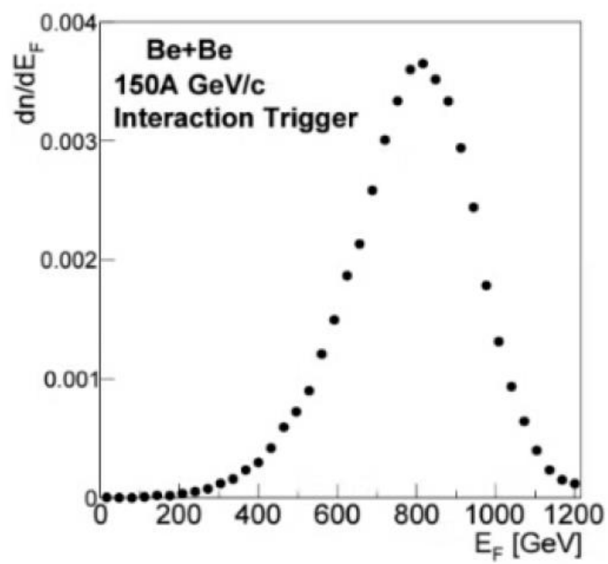


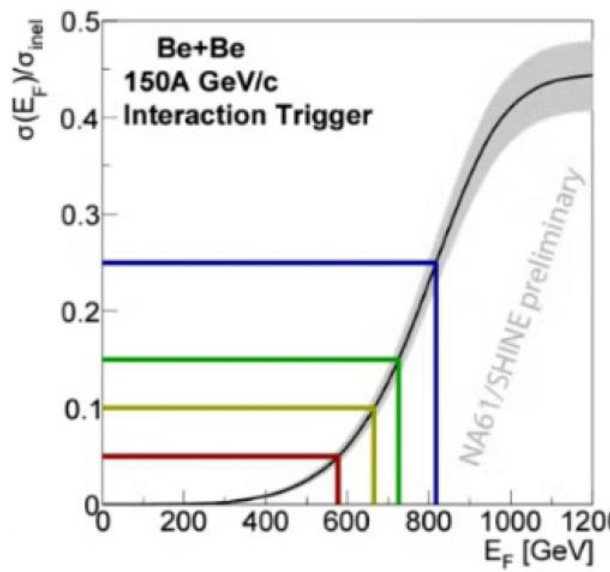

# Asymmetry in $\pi^-$ distributions in $^7Be+^9Be$

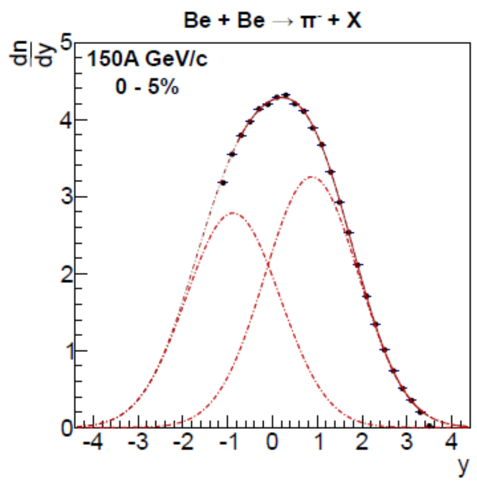


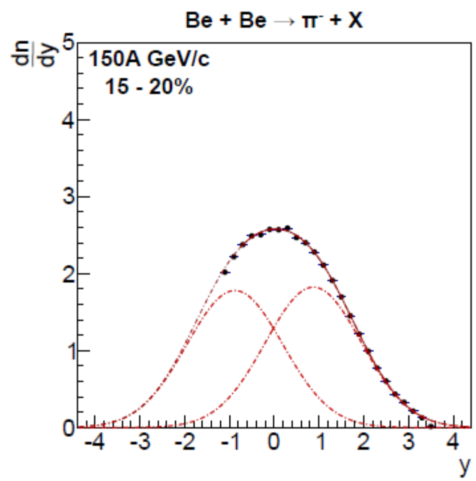


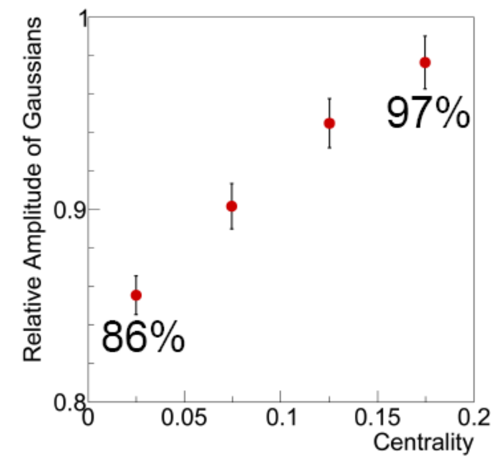


- Fitted: double Gaussian function symmetrically displaced from mid–rapidity (both Gaussians have the same width, but they differ in amplitude)
- Asymmetry decreases from 0.86 (0-5%) to 0.97 (15-20%)
- Two opposite effects influence asymmetry of the spectra:
  - asymmetric system $^7Be$ projectile on $^9Be$ target (small effect),
  - centrality selection based on projectile spectators (large effect).

# Mean multiplicities of $\pi^-$ in $^7$Be+$^9$Be

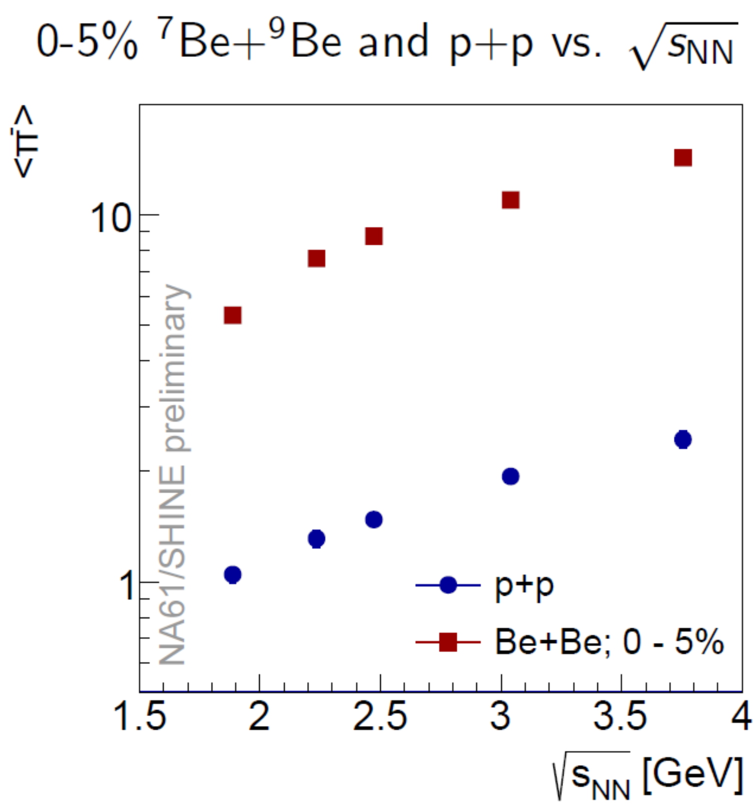


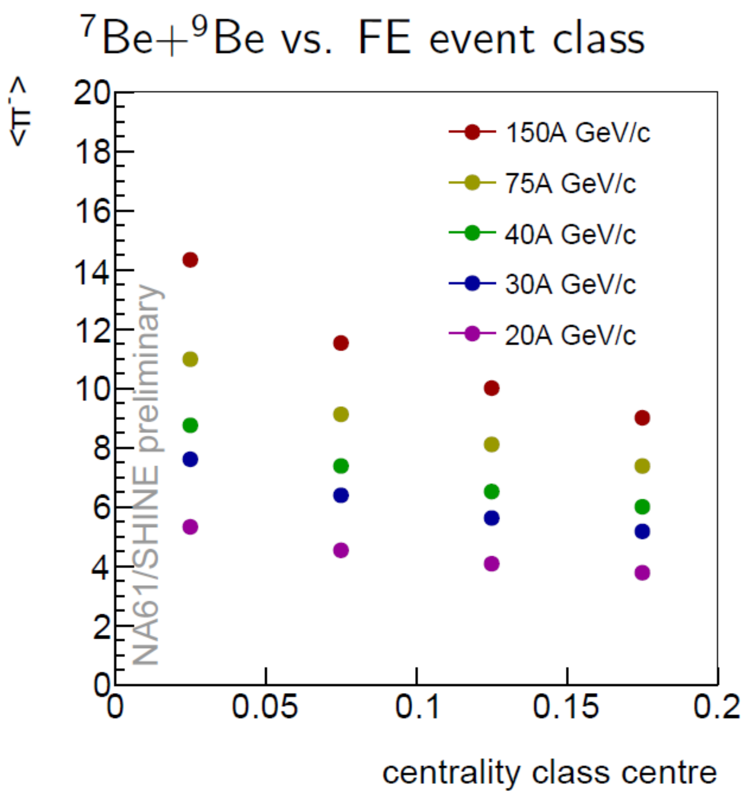


NA61/SHINE p+p results published in Eur.Phys.J. C74 (2014) 2794

# Transverse mass spectra of $\pi^-$

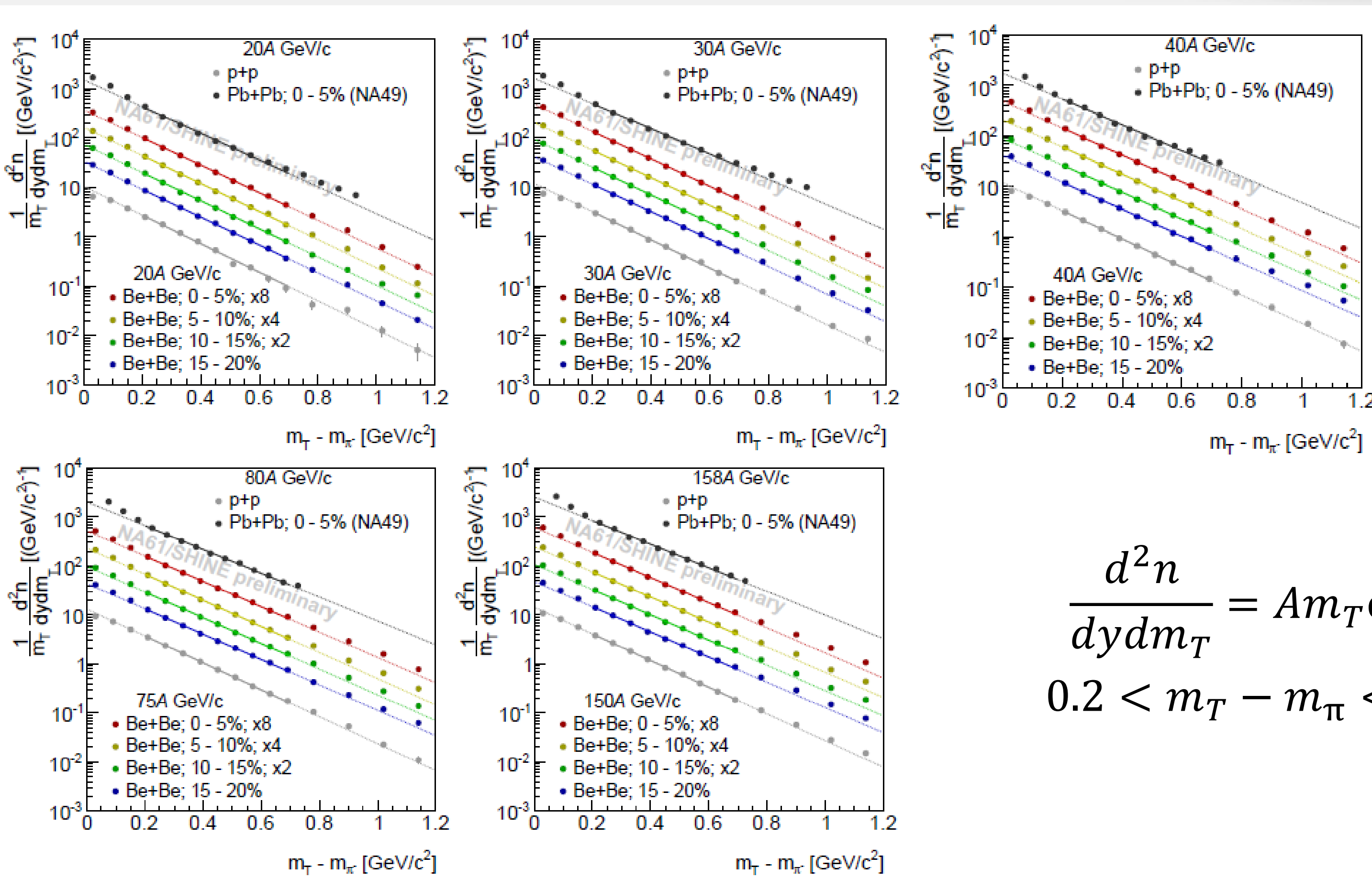


$$\frac{d^2n}{dydm_T} = Am_T\exp\left(\frac{-m_T}{T}\right)$$

$$0.2 < m_T - m_\pi < 0.7\,GeV/c^2$$

# Two-particle correlations in $\Delta\eta$, $\Delta\phi$ in p+p

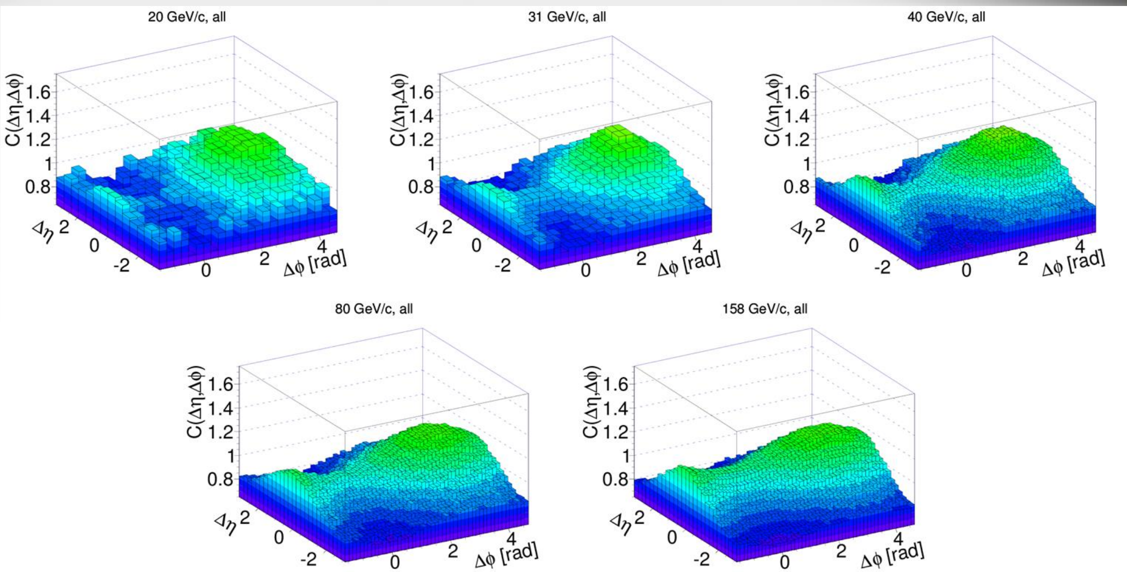


- NA61/SHINE: maximum at $(\Delta\eta,\Delta\phi) = (0,\pi)$ probably due to resonance decays and momentum conservation
- NA61 results show stronger enhancement in $\Delta\phi \approx \pi$ and no "jet peak" at $\Delta\phi \approx 0$ (in comparison with ALICE)

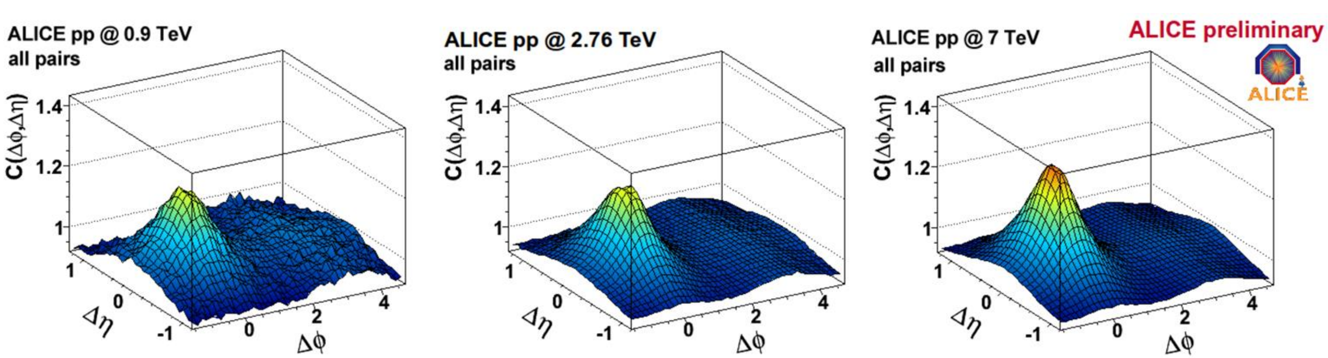

# Statistical model of the early stage

Motivation: **S**tatistical **M**odel of the **E**arly **S**tage (SMES)

Gaździcki, Gorenstein, Acta Phys. Polon. B30, 2705 (1999)

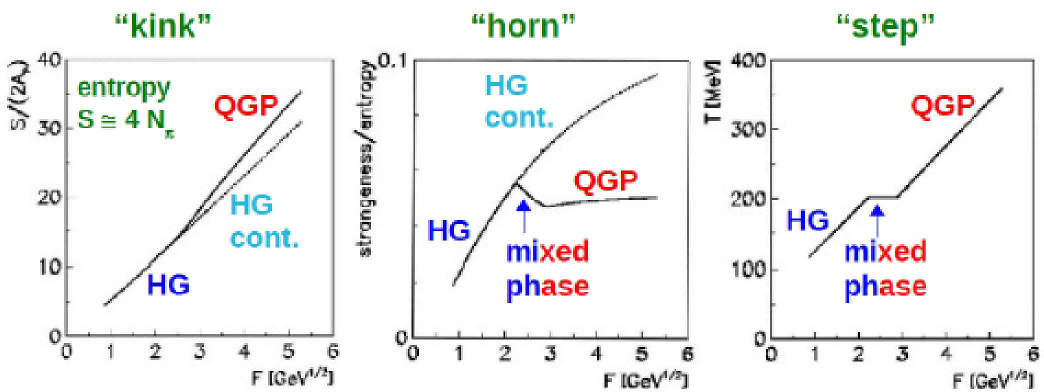


Fermi variable

$$F \equiv \left[\frac{(\sqrt{s_{NN}} - 2m_N)^3}{\sqrt{s_{NN}}}\right]^{1/4}$$

$$F \simeq \sqrt{\sqrt{s_{NN}}}$$

- 1$^{st}$ order phase transition to QGP between top AGS and top SPS energies $\sqrt{s_{NN}} \approx 7$ GeV
- number of internal degrees of freedom (*ndf*) increases HG → QGP (activation of partonic degrees of freedom)
- total entropy and total strangeness are the same before and after hadronization (cannot decrease QGP → HG)
- mass of strangeness carriers decreases HG → QGP ($m_{\Lambda, K, ...} > m_s$)
- constant temperature and pressure in mixed phase

27

# Assumptions

**main strangeness carriers**

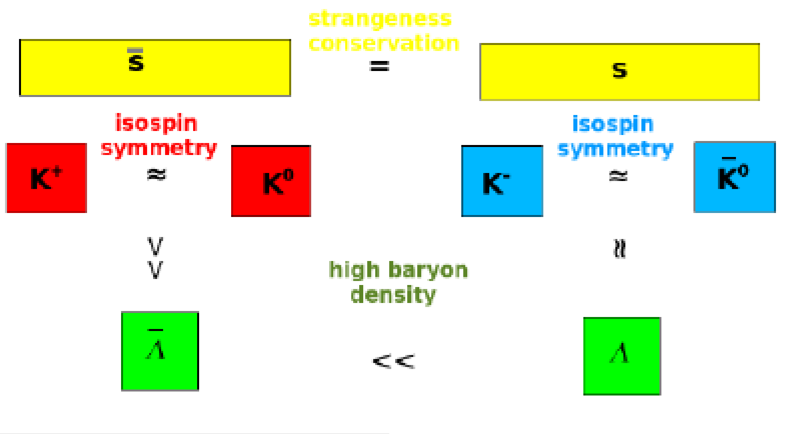


sensitive to strangeness content only

sensitive to strangeness content and baryon density

$\Lambda$ (uds)
$K^+$ (u **anty-s**)
$K^-$ (anty-u **s**)
$K^0$ (d **anty-s**)
anty-$K^0$ (anty-d **s**)

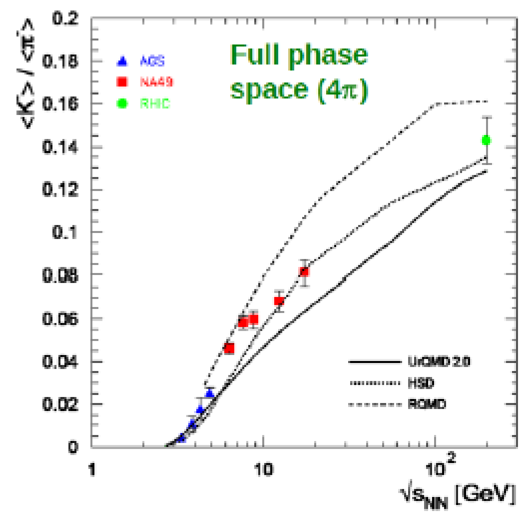


Difference in $\langle K^+\rangle$ and $\langle K^-\rangle$ production due to different sensitivity to baryon density. At SPS energies lambdas have significant influence on total strangeness production (anti-lambdas not)

$\bar{s} \rightarrow K^+, K^0$ $\quad$ **$\langle K^+\rangle/\langle\pi^+\rangle$ proportional to strangeness/entropy**

$s \rightarrow K^-, \bar{K}^0, \Lambda$ $\quad$ $\langle K^-\rangle/\langle\pi^-\rangle$ additionally sensitive to baryon density

# Scan of the phase diagram world status

## Observation of the phase transition

BNL AGS

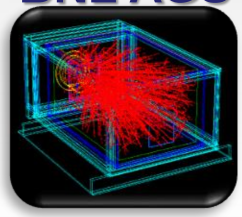

CERN SPS

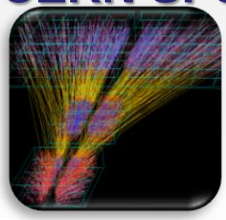

BNL RHIC

CERN LHC

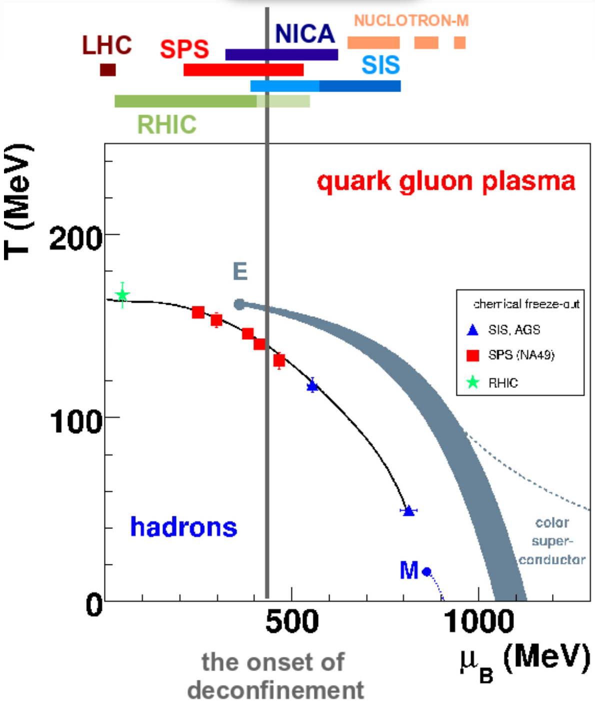


| Facility | SPS | RHIC | NUCLOTRON-M | NICA | SIS-100/300 | LHC |
|---|---|---|---|---|---|---|
| Laboratory | CERN Geneva | BNL Brookhaven | JINR Dubna | JINR Dubna | FAIR GSI Darmstadt | CERN Geneva |
| Experiment | NA61/SHINE | STAR PHENIX | BM@N | MPD | HADES + CBM CBM | ALICE ATLAS CMS |
| Start of data taking | 2009(11) | 2010 | 2015 | 2017 | 2017/18 (2019/20) | 2009 |
| cms energy [GeV/(N+N)] | 5.1 – 17.3 | 7.7 (5?) – 200 | < ~ 3.5 | 4 – 11 | 2.3 – ~4.5 ~4.5 – ~8.5 | up to 5500 14000 (p+p) |
| Physics | CP & OD | CP & OD | HDM | OD & HDM | HDM, OD & CP | PDM |

- **Strongly intensive measures Δ and Σ** (here applied to $P_T$ and N fluctuations) → PR C88, 024907, 2013
- **All NA61 results (ω[N], Δ[$P_T$, N], Σ[$P_T$, N], $\Phi_{pT}$) are corrected** for non-target interactions, detector inefficiencies and trigger bias (see talk by E. Andronov, A. Seryakov and NA61, arXiv:1510.00163)

$$\Delta[P_T,N]=\frac{1}{\omega[p_T]\langle N\rangle}[\langle N\rangle\omega[P_T]-\langle P_T\rangle\omega[N]] \qquad P_T=\sum_{i=1}^{N} p_{T\,i}$$

$$\Sigma[P_T,N]=\frac{1}{\omega[p_T]\langle N\rangle}[\langle N\rangle\omega[P_T]+\langle P_T\rangle\omega[N]-2(\langle P_T N\rangle-\langle P_T\rangle\langle N\rangle)]$$

$$\omega[P_T]=\frac{\langle P_T^2\rangle-\langle P_T\rangle^2}{\langle P_T\rangle} \qquad \omega[N]=\frac{\langle N^2\rangle-\langle N\rangle^2}{\langle N\rangle} \qquad \omega[p_T]=\frac{\overline{p_T^2}-\overline{p_T}^2}{\overline{p_T}}$$

**Δ[$P_T$, N] uses only first two moments: ⟨N⟩, ⟨$P_T$⟩, ⟨$P_T^2$⟩, ⟨$N^2$⟩**

important relation:

$$\Phi_{p_T}=\sqrt{\overline{p_T}\,\omega[p_T]}\left[\sqrt{\Sigma[P_T,N]}-1\right]$$

**Σ[$P_T$, N] uses also correlation term: ⟨$P_T$N⟩-⟨$P_T$⟩⟨N⟩**

**thus Δ and Σ can be sensitive to several physics effects in different ways**

$z_{p_T}=p_T-\overline{p_T}$ $\qquad$ $\overline{p_T}$ - inclusive average

event variable $Z_{p_T}=\sum_{i=1}^{N}(p_{T,i}-\overline{p_T})$ $\qquad$ $\Phi_{p_T}=\sqrt{\frac{\langle Z_{p_T}^2\rangle}{\langle N\rangle}}-\sqrt{\overline{z_{p_T}^2}}$